Identification of the surface state influence in representing the Arctic warming by coordinated atmosphere-only simulations

Iceberg in Greenland (Photo credit: Aline Dassel on Pixabay)

Blue-Action: Arctic Impact on Weather and Climate is a Research and Innovation action (RIA) funded by the Horizon 2020 Work programme topics addressed: BG-10-2016 Impact of Arctic changes on the weather and climate of the Northern Hemisphere. Start date: 1 December 2016. End date: 28 February 2021.

The Blue-Action project has received funding from the European Union's Horizon 2020 Research and Innovation Programme under Grant Agreement No 727852.

About this document

Deliverable: D3.1 Identification of the surface state influence in representing the Arctic warming by coordinated atmosphere-only simulations
Work package in charge: WP3 Linkages of Arctic climate changes to lower latitudes
Actual delivery date for this deliverable: Project-month 34 (30 September 2019)
Dissemination level: The general public (PU)

Lead authors
Nansen Environmental and Remote Sensing Center (NERSC): Yongqi Gao, Richard Davy, Lingling Suo
Centre National de la Recherche Scientifique (CNRS): Guillaume Gastineau
Woods Hole Oceanographic Institution (WHOI): Young-Oh Kwon
A.M. Obukhov Institute of Atmospheric Physics of Russian Academy of Sciences (IAP-RAS)ᛉ Vladimir A. Semenov
Netherlands eScience Center (NLeSC): Yang Liu

Other contributing authors
Woods Hole Oceanographic Institution (WHOI): Yu-Chiao Liang
Max Planck Institute for Meteorology (MPI-M): Daniela Matei, Rohit Ghosh, Elisa Manzini
Danmarks Meteorologiske Institut (DMI): Shuting Yang, Tian Tian
Institute of Atmospheric Physics of the Chinese Academy of Sciences (IAP-NZC): Ying Zhang
United Kingdom Research and Innovation-National Oceanography Centre (UKRI-NOC): Jennifer Mecking
Netherlands eScience Center (NLeSC): Jisk Attema and Wilco Hazeleger

Contributor outside the consortium
Istituto Nazionale di Geofisica e Vulcanologia (INGV): Annalisa Cherchi (External advisor to the project, Research and Innovation Advisory group)

Reviewer
Danmarks Meteorologiske Institut (DMI): Chiara Bearzotti

We support the Blue Growth!
Visit us on: www.blue-action.eu

Follow us on Twitter: @BG10Blueaction

Access our open access documents in Zenodo:
https://www.zenodo.org/communities/blue-actionh2020

Table of contents

Summary for publication

Arctic amplification metrics: The surface air temperature (SAT) anomalies, trends and variability have been used to quantify the Arctic amplification (AA). The use of different metrics, as well as the choice of dataset can affect conclusions about the magnitude and temporal variability of AA. We reviewed the established metrics of AA to see how well they agree upon the temporal signature of AA and assess the consistency in these metrics across commonly-used datasets which cover both the early and late 20th century warming in the Arctic. We find the NOAA 20th Century Reanalysis most closely matches the observations when using metrics based upon the trends, variability and the amplification of SAT anomalies in the Arctic, and the ERA 20th Century Reanalysis is closest to the observations in the SAT anomalies and variability of SAT anomalies. The largest differences between the century-long reanalysis products and observations are during the early warming period. In the modern warming period, the high density of observations strongly constrains all the reanalysis products, whether they include satellite observations or only surface observations. Thus, all the reanalysis and observation products produce very similar magnitudes and temporal variability in the degree of AA during the recent warming period (Davy et al., 2018).

Sea ice free Arctic contributes to the projected warming minimum in North Atlantic: Projected global warming is not spatially uniform and one of the minima in warming occurs in the North Atlantic (NA). Several models from the Coupled Model Intercomparison Project Phase 5 even projected a slight NA cooling in 2081–2100 relative to 1986–2005. Here we show that, by coupled model simulations, an autumn (September to November) sea-ice free Arctic contributes to the NA warming minimum by weakening the Atlantic meridional overturning circulation (Suo et al., 2017).

Design and finalize the set-up for the atmosphere-only model coordinated experiments: Four multi-model atmospheric coordinated experiments have been designed and finalized in order to reveal the climate impacts in the Northern Hemisphere of the warming Arctic. The atmospheric experiments will use daily SST and sea-ice concentration from 1979 to 2014 from the CMIP6 HighResMIP protocol. The first experiment uses daily varying SST and sea ice concentration. A second experiment will use varying SST while keeping climatological sea ice concentration. The difference between the two simulations will allow investigating the impacts of the warming Arctic. This protocol is built from HighResMIP and will allow investigating the influence of using high horizontal resolution. Two supplementary experiments will use daily varying SST and sea ice after removal of the multidecadal Pacific or Atlantic variability. These two experiments have never been performed before and will also allow distinguishing the specific impacts of the oceanic multi-decadal variability.

Completed the coordinated experiments by the nine of ten atmosphere-only models: All the four coordinated experiments have been completed and model outputs were made available to all Blue-Action partners.

Warm Pacific can intensify the Arctic warming: Multi-model simulations from Blue-Action showed that the transition from warm Pacific to cold Pacific (Pacific Decadal Oscillation from positive phase to

negative phase) during 1979-2013 damped the Arctic warming. The Arctic warming likely will be intensified in the forthcoming decades given the PDO switched to positive phase since 2014.

Work carried out

Arctic amplification metrics

The surface air temperature (SAT) anomalies, trends and variability have been used to quantify the Arctic amplification (AA). The use of different metrics, as well as the choice of dataset to use can affect conclusions about the magnitude and temporal variability of AA. Here we review the established metrics of AA to see how well they agree upon the temporal signature of AA, such as the multi-decadal variability, and assess the consistency in these metrics across different commonly-used datasets which cover both the early and late 20th century warming in the Arctic. We find the NOAA 20th Century Reanalysis most closely matches the observations when using metrics based upon SAT trends (A2), variability (A3) and regression (A4) of the SAT anomalies, and the ERA 20th Century Reanalysis is closest to the observations in the SAT anomalies (A1) and variability of SAT anomalies (A3). However, there are large seasonal differences in the consistency between datasets. Moreover, the largest differences between the century-long reanalysis products and observations are during the early warming period., likely due to the sparseness of the observations in the Arctic at that time. In the modern warming period, the high density of observations strongly constrains all the reanalysis products, whether they include satellite observations or only surface observations. Thus, all the reanalysis and observation products produce very similar magnitudes and temporal variability in the degree of AA during the recent warming period (Davy et al., 2018).

Sea ice free Arctic contributes to the projected warming minimum in North Atlantic

Projected warming is inhomogeneous over the globe. The North Atlantic Ocean is one of the regions with minimum projected warming according to climate model projections. Several models from the Coupled Model Intercomparison Project Phase 5 (CMIP5) even projected a slight cooling in 2081-2100 relative to 1986-2005 for the North Atlantic Ocean. By series of numerical model simulations using both the Bergen Climate Model (BCM) and the atmospheric component of BCM, it is found that the sea-ice free Arctic contributes to the projected warming minimum in the North Atlantic.

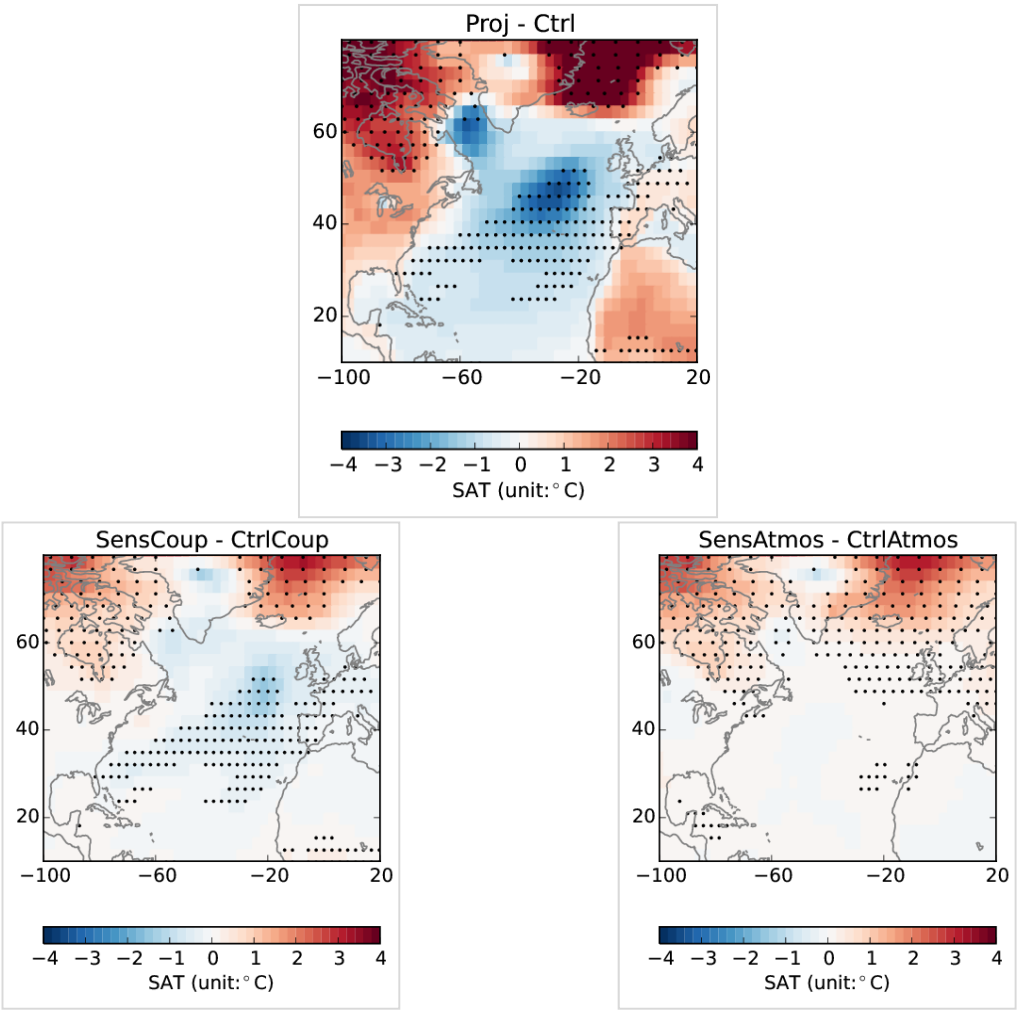

Figure 1 Simulated annual mean changes in surface air temperature with BCM. a) between the future projection (Proj) during the Arctic sea ice free period and the present-day climate (Ctrl), b) in response to the sea-ice free Arctic with BCM, c) in response to the sea-ice free Arctic with atmospheric component of BCM. The dots in a, b and c) show where the responses simulated with BCM / ARPEGE pass the 95% significance test.

Suo et al. (2017) describe the mechanism causing the slow-down of the projected warming of the North Atlantic by the fact that the autumn sea-ice free conditions in the Arctic triggers a weaker Icelandic low during autumn. This is further associated with the weakened wind stress over the subpolar gyre reducing the intensity of the deep convection over the subpolar north Atlantic and accordingly contributing to a weakening of the Atlantic meridional overturning circulation (AMOC). The weakened AMOC leads to a decrease in northward heat transport and a cooling of the ocean surface in the mid-latitude of the North Atlantic. The role of air-sea interaction in the response to changes in the Arctic sea ice extent (see figure 1), which so far has not been widely discussed in the literature, has been highlighted by the results presented in this paper.

Re-design and finalize the set-up for the atmosphere-only model coordinated experiments

The following Atmospheric General Circulation Model (AGCM) coordinated experiments were finalized: Exp1: Daily sea ice concentration (SIC) and sea surface temperature (SST) from 1979 to 2014; Exp2: daily SIC climatology in Arctic or Northern Hemisphere (mean of 1979 to 2014) and daily-varying SST from 1979 to 2014; Exp3: daily-varying SIC from 1979 to present and time-varied daily SST (1979 to 2014) with Interdecadal Pacific Variation (IPV) signal removed in Pacific (25^{o}S-60^{o}N) (25^{o}S-Bering Strait) (Transition zone: 35^{o}S to 25^{o}S in Pacific sector); Exp4: daily-varying SIC from 1979 to present and time-varied daily SST (1979 to present) with Atlantic Multi-Decadal Variation (AMV) signal removed in North Atlantic (0-60^{o}N) (tropical-Greenland-Iceland-Scotland Ridge)(Transition zone: 10^{o}S-0 in Atlantic sector). The experiments were designed to address the impact of the Arctic sea ice change (Exp1 minus Exp2), the impact or modulation of IPV (Exp1 minus Exp3) and the impact or modulation of AMV (Exp1 minus Exp4). The external forcing will be the CMIP6 forcing and the boundary SIC and SST are HadISST 2.2.0.0. (Titchner and Rayner, 2014). The IPV and AMV follows the estimation distributed through DCPP-CMIP6 (Boer et al., 2016). The SST and SIC will be adjusted following Hurrel et al. (2008) to ensure consistency between the two surface fields.

CNRS also compared the AMV and IPV amplitude from the DCPP CMIP6 panels to alternative estimations. The AMV and IPV are estimated using statistical techniques that evaluate the amplitude of external forcing (greenhouse gases and aerosols) impacts onto the SST. The AMV and IPV are estimated using the residual SST once the external forcing is removed. DCPP CMIP6 used signal to noise empirical orthogonal function using models and observations (updated from Ting et al., 2009). CNRS has compared those estimations to those obtained using alternate techniques that on rely on observations (Frankignoul et al., 2017). Among those techniques, removing the global mean SST uniformly is commonly used (Trenberth and Shea, 2006). It was found that a linear inverse modelling (LIM) optimal filter provide the best estimation of the influence of external forcing. The IPV and AMV amplitudes are compared in figure 2. The IPV was calculated using Henley et al. (2015), while the AMV is the SST average over 0°N-60°N 70°W-5°W. The IPV amplitude seems robust among the different statistical techniques. The AMV time series show more difference among members, with the AMV produced by the LIM optimal filter having lower AMV values from 1979 onward. However, the time variability of the AMV and IPV is consistent among all estimations.

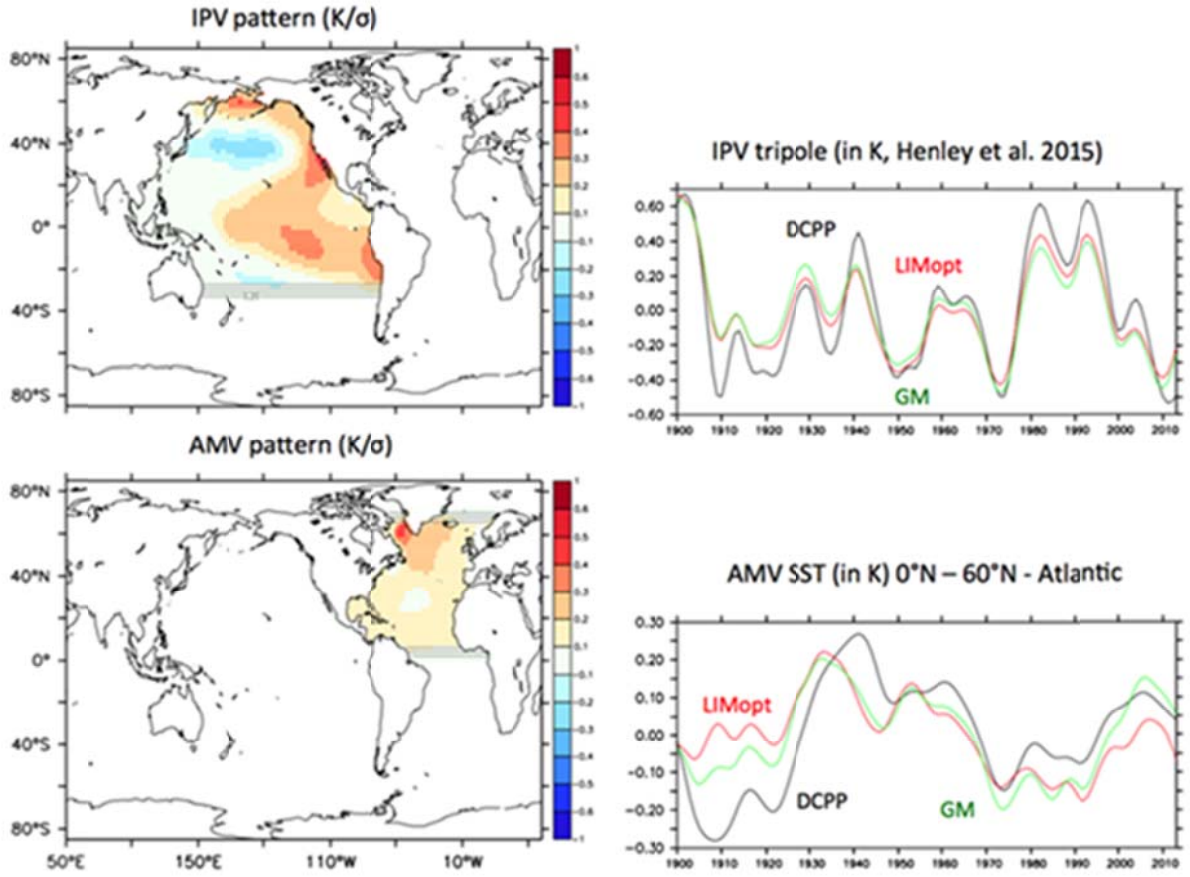

Figure 2 Main mode of SST decadal variability (Top-left) Interdecadal Pacific variability (IPV) and (Bottom-left) Atlantic multidecadal variability (AMV) patterns, in K for one standard deviation of the normalized indices. (Top-right) IPV tripole, defined as in Henley et al. (2015) and (Bottom-right) AMV, defined as the mean Atlantic SST in 0°N-60°N, in the (black) DCPP, (red) the HadISST data analysed with a linear inverse modelling optimal filter and (green) the HadISST data with a removal of the global mean SST.

The removal of PDO/AMO signal in the HadISST2.0.0 data was done using the yearly indices and the patterns, linearly interpolated onto the daily and horizontal high-resolution grid. CNRS made the boundary forcing for Exp3 and Exp4 available for the nine modelling groups.

We have assessed the quality of the atmospheric experiment forcing fields. The HighResMIP surface boundary conditions were first evaluated against other observation estimates. The sea ice extent that is used in the Blue-Action experiments is comparable to other observational estimates in terms of trends and interannual variability, even if we note a mean state biased toward a larger sea-ice extent. The coordinated experiments also use estimations of the natural Atlantic and Pacific multidecadal variability that rely on estimates of the impacts of anthropogenic and external forcing. We found that such estimates are robust for the Pacific Ocean, but sensitive to the method used in the Atlantic Ocean (Frankignoul et al., 2017).

Completed the coordinated experiments by the nine of ten atmosphere-only models

The coordinated experiments have been completed by nine (NERSC, CNRS-LOCEAN, DMI, CMCC, IAP-NZC, UoS, MPIM, NLeSC, WHOI-NCAR) of the ten modelling groups, including Chinese (IAP-NZC) and US (WHOI-NCAR) partners. Every modelling group made their simulation outputs available to all WP3 partners. Several joint analysis groups have been established with the identified leading scientist.

Results based on Blue-Action multi-model simulations

1) **Sea-ice influence in the coordinated experiments** (Leading partner: CNRS)

1.1 Long-term trends in surface warming and large-scale atmosphere circulation

The sea-ice influence was evaluated with the winter (December-January-February: DJF) trend eight of the nine coordinated simulations, for which the data were available when analysis started. The sea-ice influence was calculated with the difference of the Exp1 and Exp2 ensemble mean simulations (see figure 3). We also computed the sea-ice influence in the multi-model ensemble average, to remove the influence of internal variability. we calculate the mean of the 145 members available from these simulations (figure 3, bottom right). The statistical significance was established using student t-test for individual models, while the trend of the multi-model mean was calculated assessing where at least 7 models (out of 8) show a trend of the same sign, which corresponds to a p-value of 10.9% with a binomial law (n=8, p=0.5).

Most simulations show negative sea level pressure (SLP) DJF anomalies above the region of sea-ice retreat, such as above the Barents, Labrador and Okhotsk Seas. These negative SLP anomalies are consistent with the hydrostatic response to low-level warming. We also distinguish a large scale SLP pattern in the Eastern Atlantic and western Europe, with positive SLP anomalies above Iceland and the Nordic seas and negative anomalies over western Europe, so that it resembles the negative phase of the North Atlantic Oscillation (NAO). The amplitude of the simulated trend is of the order of 1 K and 0.5 hPa per decade over the sea-ice edge, and 0.1 K and 0.1 hPa within the midlatitude. Such a pattern is, therefore, lower than observed changes where the internal variability might dominate (Ogawa et al., 2018). However, the overall pattern of the multi-model mean share some similarity with the observed changes, as both show a tendency toward negative NAO-like anomalies. We did not find any significant cooling over Siberia, unlike observations that show a tendency toward a warm Arctic Cold continent pattern. However, the negative NAO-like pattern induces warming in the eastern Mediterranean region and cooling over south-western Europe. An insignificant cooling is also observed in North America.

There is, therefore, a discrepancy of our results with Ogawa et al. (2018) regarding the negative NAO-like pattern. Indeed, Ogawa et al. (2018) found in similar coordinated experiments a weaker SLP pattern with no SLP anomalies over western Europe. We speculate here that the differences might come from the different boundary conditions used for SST and SIC, as there are substantial observational uncertainties remain. The differences might also come from the experimental protocol, as the influence of external forcing was not removed in the simulations of Ogawa et al. (2018), when compared to the results presented here.

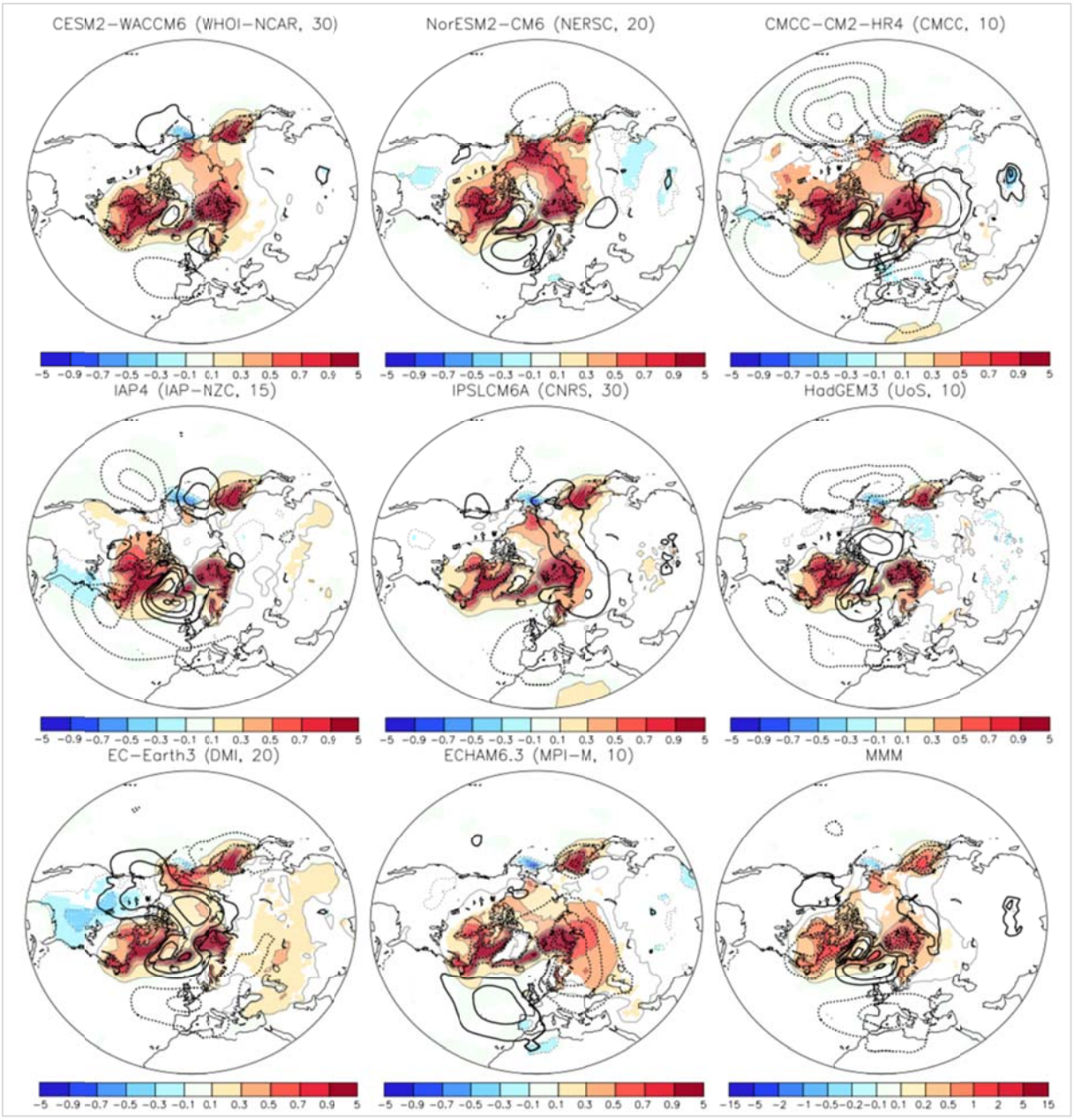

Figure 3 Surface air temperature (T2m) trend in 1979-2014 of Exp1 minus Exp2 in Blue-Action WP3 models, in K decade-1 (color) and associated SLP trend, in hPa decade^{-1} (contour, CI 0.2 hPa decade-1 for individual models and 0.1 hPa decade-1 for the MMM). MMM indicate the multi-model trend, and is shown with a color bar different from that of individual models. Colors are masked if statistical significance is above 5% for the student t-test of the ensemble means. Colors in the multi-model trend map indicate where at least 7 models show anomalies of the same sign.

1.2 Interannual variability

The interannual sea ice influence was further investigated using a maximum covariance analysis (MCA) between Arctic sea ice concentration and SLP, after removal of a quadratic trend for both fields. The MCA provides the main mode of covariability between two fields (Frankignoul et al., 2011), and the level of statistical significance was established using 100 random resamplings of the SLP field, with repetition. Additionally, two statistics can provide estimations of the covariability, the correlation between the time series (R) and the square root of the normalized squared covariance (NSC, eigenvalue of the covariance matrix divided by the variance of both fields). We used the monthly SIC boundary conditions of Exp1 as a left field, and the DJF SLP difference of Exp1 minus Exp2 multi-model mean of the eight models (see figure 3 for the models used) as a right field. This multi-model mean was calculated with the mean of the 145 members.

The MCA results did not indicate any significant mode of covariability when the SIC lead the atmosphere by one, two or three months, or when the SIC is simultaneous. The first MCA mode when the SIC leads the atmosphere (see figure 4) is a dipole of SIC anomalies with an opposite sign over the Labrador Sea and the Greenland/Barents sea, inducing positive (negative) SLP anomalies over positive (negative SIC anomalies). The SIC anomalies might reflect the influence of the NAO onto the sea ice found in observations (Frankignoul et al., 2014), and the response obtained seems mainly due to the localized lower-tropospheric warming (cooling) where the sea ice melted (expanded). The second MCA mode corresponding to the February (L=0, not shown) or January (L=1) show a similar localized SLP response to sea ice changes, but for negative SIC anomalies over the Arctic except for the Greenland Sea when positive SIC anomalies occurred. However, for the December (L=2) sea ice and DJF atmosphere, the MCA shows that decreasing sea ice in the Greenland and Barents Seas, together with increasing sea ice in the Labrador Sea is followed by an intensification of the Siberian High and Aleutian Low. When considering the November SIC (L=3) similar patterns are found. Therefore, the coordinated simulations reproduce somehow the covariability found previously in observations between the AO and the sea ice in the Barents-Kara region (King et al., 2014; Kug et al., 2014), however the sea-ice pattern forcing the AO is more complex. Interestingly, we note a correlation of R=0.70 between the atmospheric and SIC time series for SLP in DJF and sea ice in November. Nevertheless, the amplitude of the pattern is about 0.1hPa, and it therefore 10 times weaker than observations.

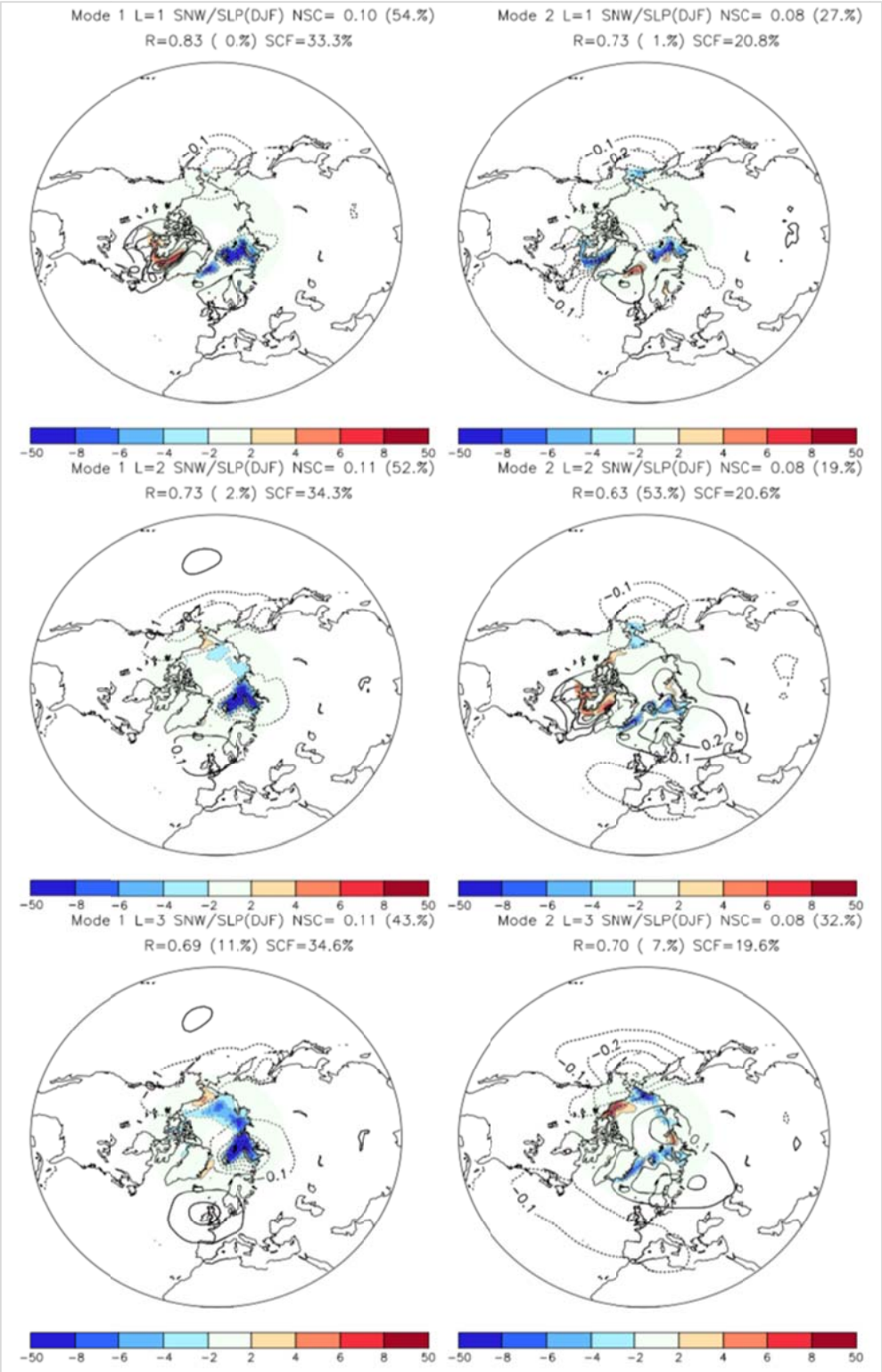

Figure 4 Sea ice concentration (in %) used as boundary condition and DJF SLP (in hPa) of ALL - NoSIC covariance map, for the (left) first and (right) second MCA mode of the multi-model mean. The sea ice concentration is in January (L=1, top), December (L=2, center) or November (L=3, bottom). The

homogeneous (heterogeneous) map is shown for SIC (SLP). The square root normalized square covariance (NSC), correlation (R) and square covariance fraction (SCF) are indicated on top of each panel, together with the p-value associated with NSC and R, in %.

2) Links between the surface state and the continental snow cover

The snow cover was found to influence climate during fall in observation and coupled climate models (Gastineau et al., 2017). In both cases, the sea ice is associated with the continental snow cover, so that it is difficult to distinguish the snow and sea-ice influences. The continental snow cover also has important impacts in spring (Zhang et al., 2004; Peings et al., 2011). These two seasons also show the largest decreasing trend in the recent period (Mudryk et al., 2017). Therefore, we used the atmosphere-only experiments to evaluate the role of snow cover and to evaluate the links between snow cover in fall (November) and spring (April) and Arctic sea ice. We first evaluate the mean snow cover simulated by models and compared it to ERAInterim-I. Figure 5 shows the climatological variations of the land area covered by snow. The climatological snow cover is realistic in most models. Nevertheless, we note that ECHAM6 underestimates the snow cover in Eurasia and North America. IPSL-CM6A underestimates the snow cover over North America, while IAP4 overestimates it.

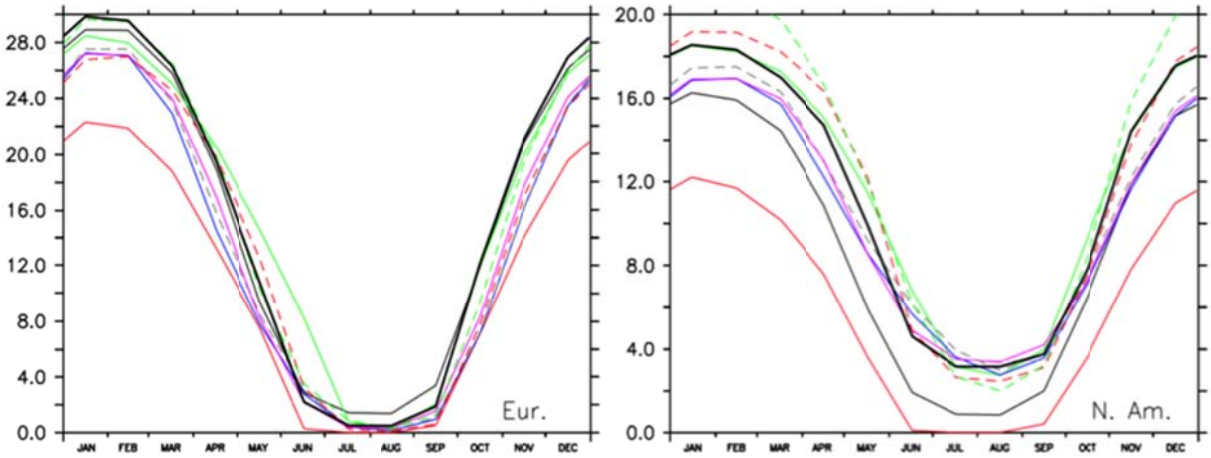

Figure 5 Climatological snow-covered area over (left) Eurasia and (right) North America, in 10^6 km^2, in the Blue-Action simulations. Thick black: ERA-Interim; black: IPSLCM6A; red : ECHAM6; green : EC-Earth; blue : NorESM2; purple : CMCC2; dash grey : CESM2; dash green : IAP4; dash red HadGEM3.

To determine the respective influences of (1) the SST, external forcing and Southern Hemisphere sea ice (referred to as SST/Ext in the following), and (2) Arctic sea ice, we performed a two-way analysis of the variance (ANOVA) based on the snow cover field. We used the eight models illustrated previously. The effect of SST/Ext is quantified by the difference of snow cover when comparing each year of Exp2, while the effect of Arctic SIC is given by the difference between Exp1 and Exp2. The influence of the interaction between the SIC and SST/Ext effects can also be quantified. The results (see figure 5) show that most of the variance is explained by SST/Ext, with a significant influence on the snow cover field. The influence of the SST/Ext is larger in spring than in fall in northeastern Europe and North America,

with influence over the edge of snow-covered land. A large SST/Ext influence is also found over the Tibetan plateau in both fall and spring. The SIC or the interaction terms do not find a robust influence (see the p-value indicated in figure 6). We also analyse the models separately, which reveals some localized SIC influence, but it is not robust among models. The largest influence is localized in North-Eastern Europe, over Finland, northwestern Russia and western Canada. The SIC influence is larger in fall, as expected from the warming trends, and the larger polar amplification during this season.

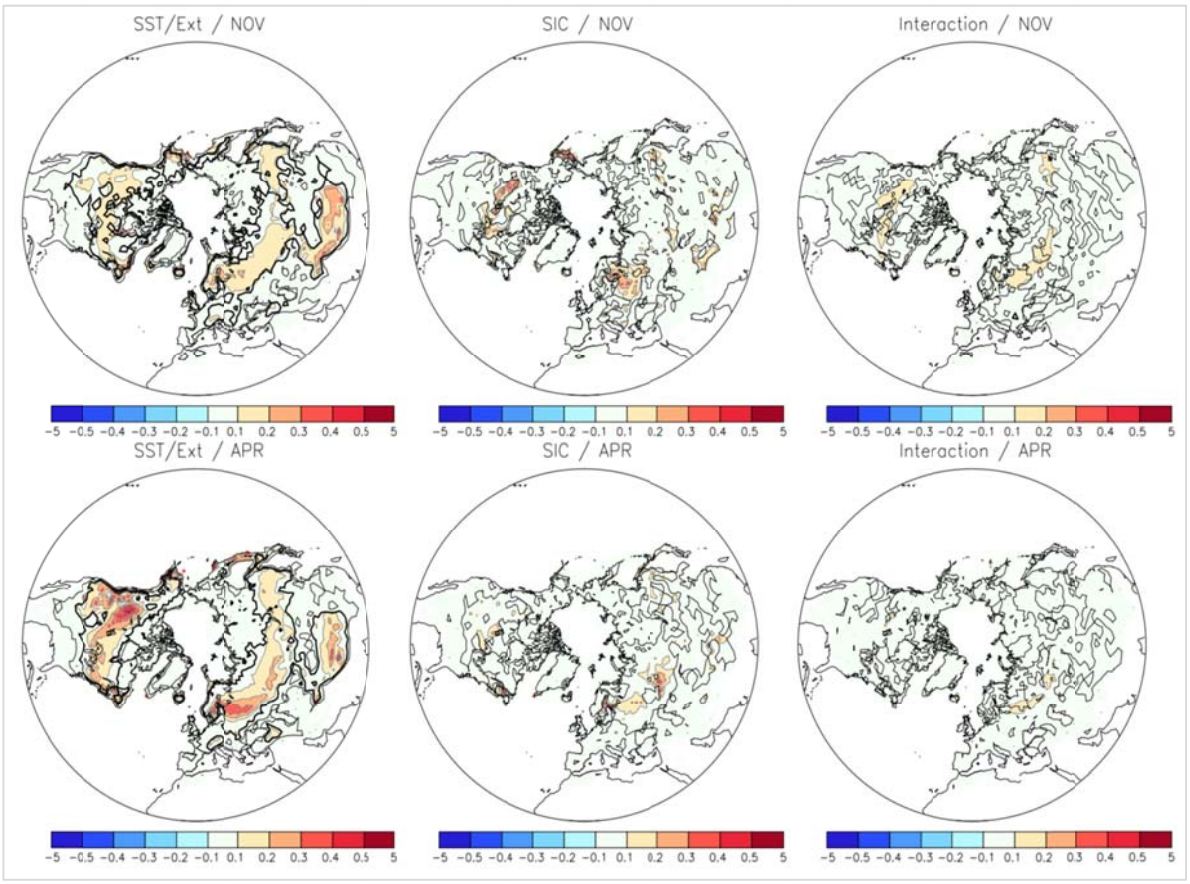

Figure 6 Mean square of the continental snow cover (in %^{2}) associated to the (left) SST/Ext, (center) SIC and (right) interaction term in the two-way ANOVA, for (top) November and (bottom) April. The thick black line indicates when the p-value of the ANOVA test is below 10% for at least 4 models. The thin black line indicates when this p-value is below 10% for at least one model.

The main mode of snow cover variability associated to the SST/Ext, SIC and internal variability was further characterized in the eight models using empirical orthogonal function (EOF) of the snow cover field in (1) the ensemble mean Exp2 for SST/Ext, (2) the difference of the ensemble mean Exp1 minus Exp2 for SIC and (3) the residue after removal of the ensemble mean for the internal variability. The first EOF (figure 7) of all models is similar (not shown) and has large loading south of Scandinavia, in northwestern Russia for the influences for SST/EXT, SIC or internal variability. In fall for all factors or in

spring for SIC, we also find snow cover anomalies of the same sign over North America. In spring the SST/Ext factor is also associated with anomalies of the opposite sign over North America. In fall the SIC is associated with a decrease of snow cover over eastern Russia.

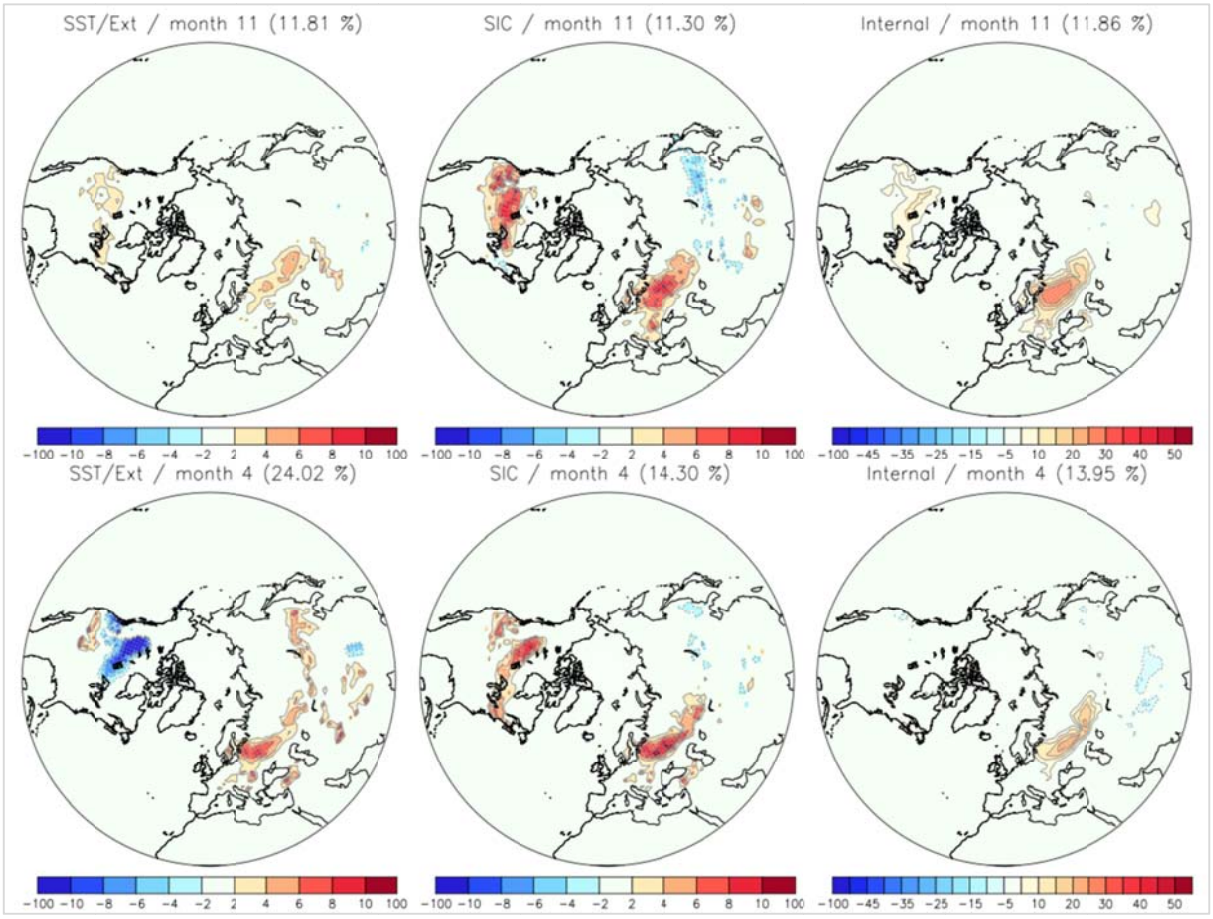

Figure 7 First EOF of the continental snow cover (in %) associated with (left) SST/Ext, (center) SIC and (right) internal variability in (top) November and (bottom) April. The patterns shown are the mean EOF of the eight models, calculated to provide positive snow cover anomalies over eastern Europe.

Lagged regression using the principal component associated with the EOF shown in figure 7 can be used to explain the generation of the snow cover anomalies associated to each climate factors (SST/Ext, SIC and internal variability), and to investigate the role of the snow cover and its links with the SIC or the SST/Ext. The regression analysis was performed in a preliminary analysis using six of the eight models used, after excluding IPSLCM6A and CESM2 for technical reasons. We found that the fall snow cover anomalies are associated with almost little air temperature (T2m for 2m temperature) or SLP anomalies for SST/Ext and SIC. Most of the snow cover impact might therefore by induced by the advection by the mean flow of cold SST over North Atlantic or North Pacific (figure 8, upper-left) or increased SIC over the Barents/Kara seas (figure 8, upper center). We note the occurrence of an anticyclone over the Aleutians consistent with reduced sea ice over the Chukchi Sea, which can explain the associated cold anomaly and increased snow cover over North America. In contrast, the internal

variability (figure 8, upper right) show the influence of the Ural anticyclone and Scandinavian blocking onto the snow cover, as previously found in Gastineau et al. (2017). In spring, the snow cover anomalies are mainly related to the influence of the atmosphere with a lag of one month. The snow cover anomalies explained by El Niño Southern Oscillation and the associated teleconnection for the SST/Ext factor (figure 8, bottom-left). The SIC factor illustrates the influence of a warm Okhotsk sea. The main internal mode of variability acting on the snow cover is the Scandinavian pattern, with a large anticyclone over Northern Europe inducing a large cooling over Eurasia in both fall and spring.

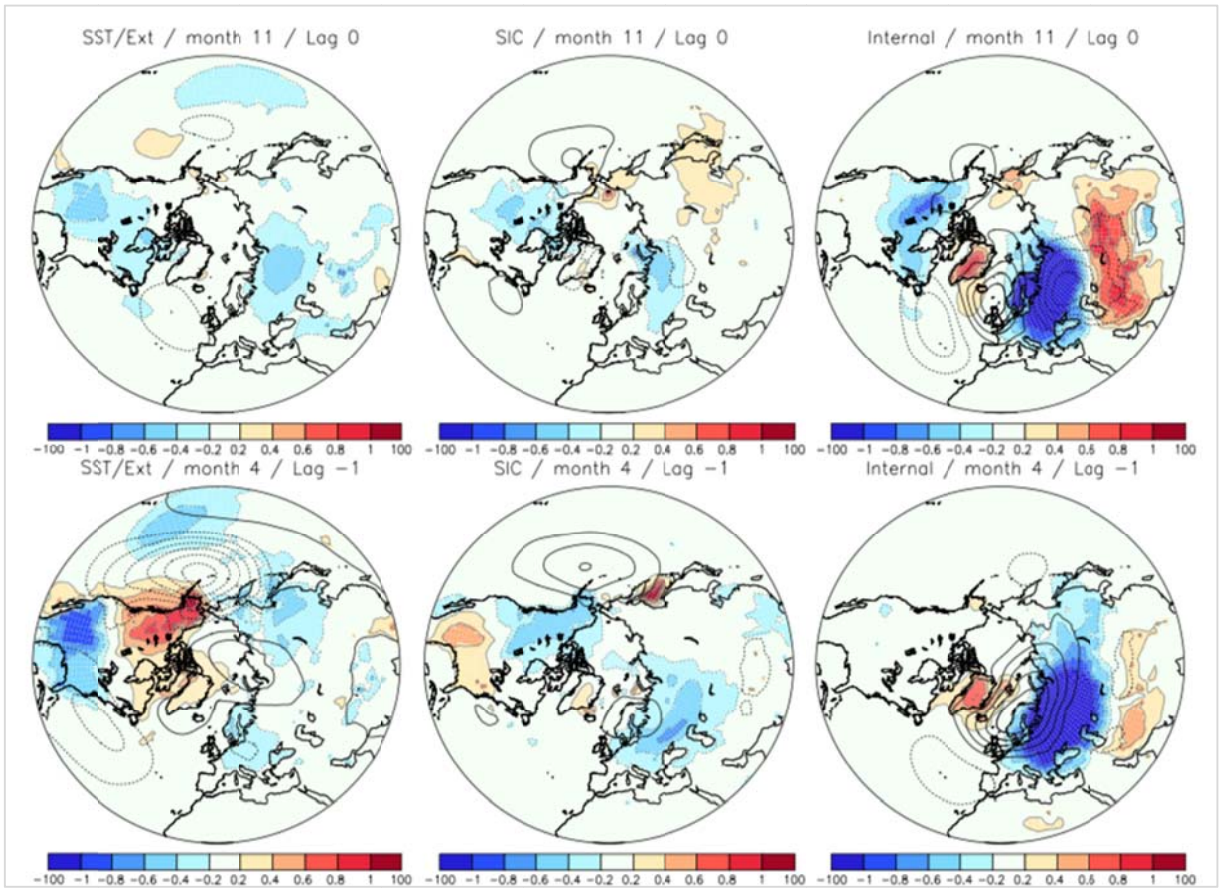

Figure 8 Lagged regression of the T2m (colors, in K) and SLP (contour, CI=0.5 hPa) onto the PC1 associated with the (Left) SST/Ext (center) SIC and (right) internal factors, for (first line) the atmosphere in November associated with the PC1 of November snow cover, (second line) the atmosphere in March leading the PC1 of April snow cover and (third line) the atmosphere in January lagging the PC1 of November snow cover. The patterns shown are the multi-model mean of the regressions obtained separately with six models (ECHAM6, EC-Earth, NorESM2, CMCC2, IAP4, and HadGEM3).

Interannual variability of the Arctic sea ice-driven atmospheric circulation: Mechanism and Impacts (Leading partner: WHOI)

To understand how the sea ice drives interannual atmospheric circulation variability in wintertime and what are the associated impacts, the Exp1 and Exp2 are analyzed. We remove the quadratic trends from

all the variables to concentrate on the interannual variability. The leading modes of sea ice-driven winter SLP variability from seven models commonly show an annular shape with one sign over the Arctic and the opposite sign in the midlatitude, explaining 30-44% of the total sea-ice driven variance (figure 9). The sea ice concentration pattern that drives the EOF1 SLP anomalies with high pressure center over Northern Eurasia exhibits enhanced sea ice in the Nordic and Barents Seas (figure 10a). Consistent with the sea ice and SLP patterns, the near surface air temperature exhibits broad regions of cold anomalies from Nordic/Barents Seas to Siberia (figure 10b). This relationship for the interannual variability is different from the so-called warm Arctic – cold Eurasia pattern suggested by some studies for the long-term trends. Preliminary results for the mechanism responsible for this relationship suggest there are different mechanisms between early and late winter. The associated precipitation anomalies show overall drying in the colder air temperature region, associated with reduced stormtrack and enhanced blocking activities (figure 10c-e).

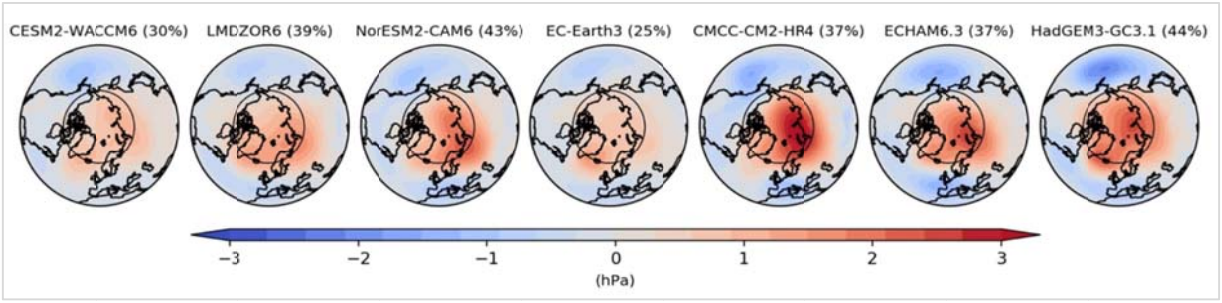

Figure 9: The leading EOF mode of the sea ice-driven winter (DJF) SLP variability from each model. Quadratic trends are removed at each location prior to the EOF calculation to only include the interannual to decadal variability. The percentage of total variance of sea ice-driven winter SLP variability explained by the first EOF mode is indicated in the parentheses.

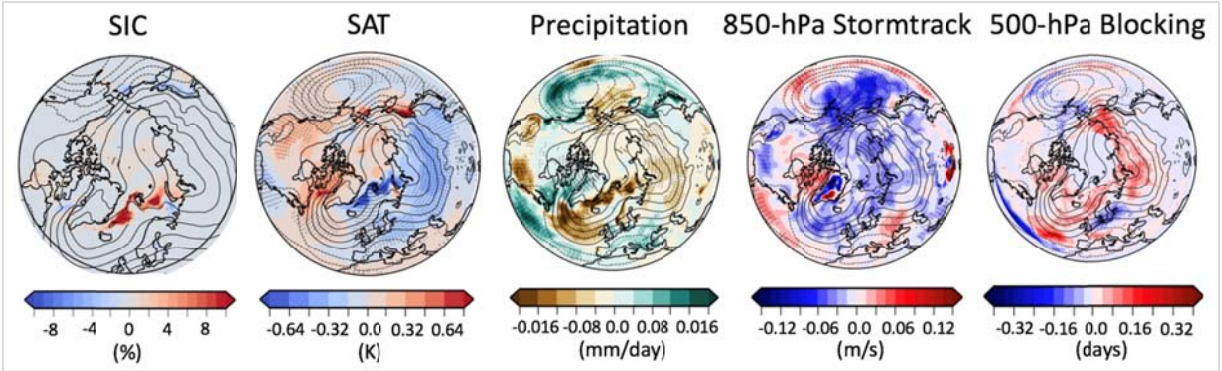

Figure 10: Regressions on the leading principal component time series of the sea ice-driven winter SLP variability for (a) sea-ice concentration, (b) near-surface air temperature, (c)precipitation (including both rain and snow), (d) 850 hPa storm track (defined as the standard deviation of 2-6 day band-pass filtered meridional wind), and (e) the number of blocking days (defined using daily 500 hPa geopotential height).

The regression of sea ice-driven winter SLP variability is also plotted in each panel with the contours. Only the WACCM6-SC 30 member ensembles are used for this plot.

Change of sea ice, PDO and AMO contribute to the Arctic warming (Leading partner: NERSC)

Figure 11 shows the Arctic temperature trend from 1979 to 2013 in a) ERAInterim and b) multimodel simulations from Blue-Action WP3 Exp1. The simulations partly reproduced the Arctic warming in mid-lower troposphere with the strongest warming in near surface during autumn. Warming aloft is also partly reproduced except the warming above 300hPa in Jan-Feb.

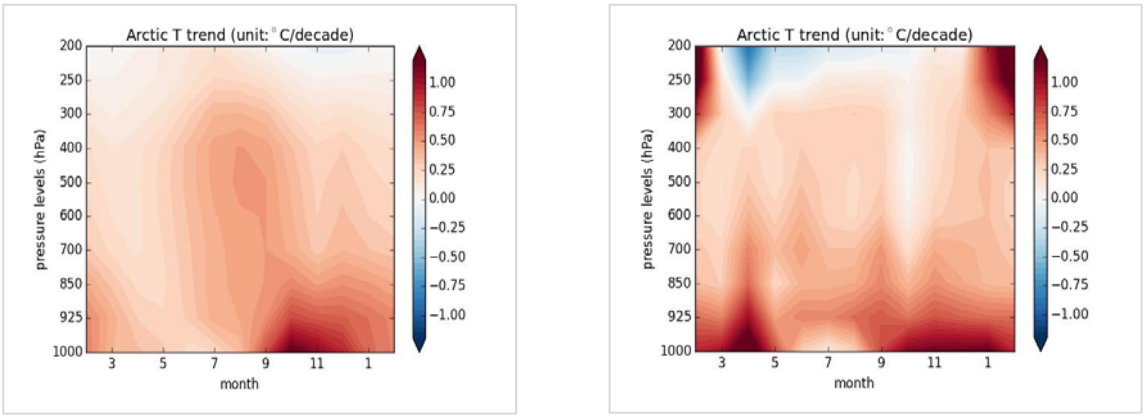

a) b)

Figure 11 The Arctic temperature trend from 1979 to 2013 in a) ERAInterim and b) multimodel simulation. The models employed include EC-EARTH3 with 20 ensembles, IAP4 with 15 ensembles, IPSL-CM with 30 ensembles, and NorESM2 with 20 ensembles.

Figure 12 shows the Arctic sea ice, PDO, and AMO impact on the Arctic warming trend from 1979 to 2013. The Arctic sea ice loss contributed most of the near-surface warming during the autumn, and also partly contributed to the warming up to 400hPa in February. However, the contribution to the warming above 850hPa is insignificant except February. The contribution of AMO to the Arctic warming trend is weak and is not statistically significant. The contribution of PDO damped the Arctic warming trend during 1979-2013 significantly in spring, autumn and early winter from the near-surface to the upper troposphere. The reduction of warming reaches 0.3/0.2 °C per decade in the upper/lower troposphere. Further analysis will be performed to find out the underlying mechanisms. Since the PDO is in transition from the positive phase to the negative phase during 1979-2013, this implies that the positive phase of PDO can intensify the Arctic warming, consistent with Svendsen et al. (2018) and opposite to Screen et al. (2016). The PDO switched to the positive phase since 2014, our results also suggest that the Arctic warming will be intensified in the forthcoming decades if other forcings are unchanged.

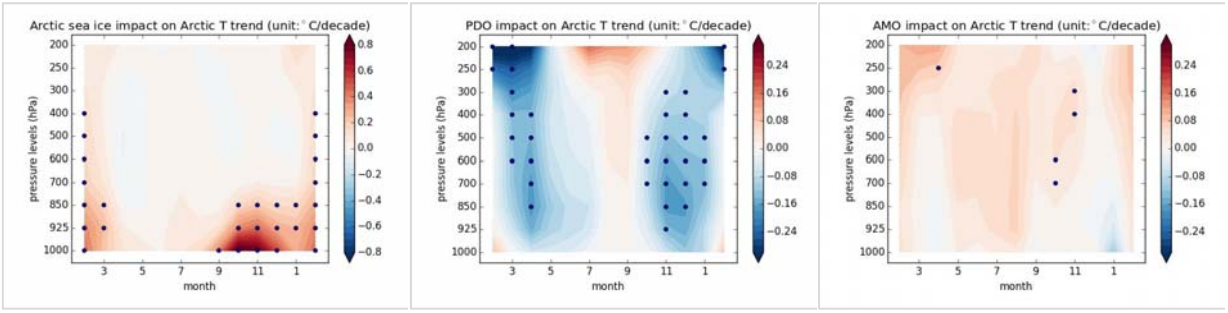

a) b) c)

Figure 12 Multimodel mean of the differences in the Arctic temperature trend from 1979 to 2013 between the historical simulation (Exp1) and a) Arctic sea ice climatological simulation (Exp2), b) NOPDO simulation (Exp3), and c) NOAMO simulation (Exp4). The models used include EC-EARTH3 with 20 ensembles, IAP4 with 15 ensembles, IPSL-CM with 30 ensembles, and NorESM2 with 20 ensembles. The blue dots mark the differences pass the 95% statistical significance test.

Meridional Energy Transport from Midlatitudes to the Arctic (Leading partner: NLeSC)

We calculated atmospheric meridional energy transport (AMET) using the coordinated experiments by 9 atmosphere only models. The AMET is taken as the residual between net surface turbulent and radiation fluxes and net radiation fluxes at the top of the atmosphere. All the members from 4 experiments by each atmosphere-only model simulations are included.

We compared AMET in Exp1 and Exp2 to investigate the influence of sea ice variations on heat transport. In addition, AMET estimated from Exp3 and Exp4, in which the PDO and AMO were removed, will be compared with those from Exp1 to illustrate the impact of PDO and AMO on energy transport. Moreover, the changes of surface turbulent fluxes due to the presence of fixed sea ice, removal of PDO and AMO compared to varying sea ice are investigated with respect to their spatial structure in the Arctic.

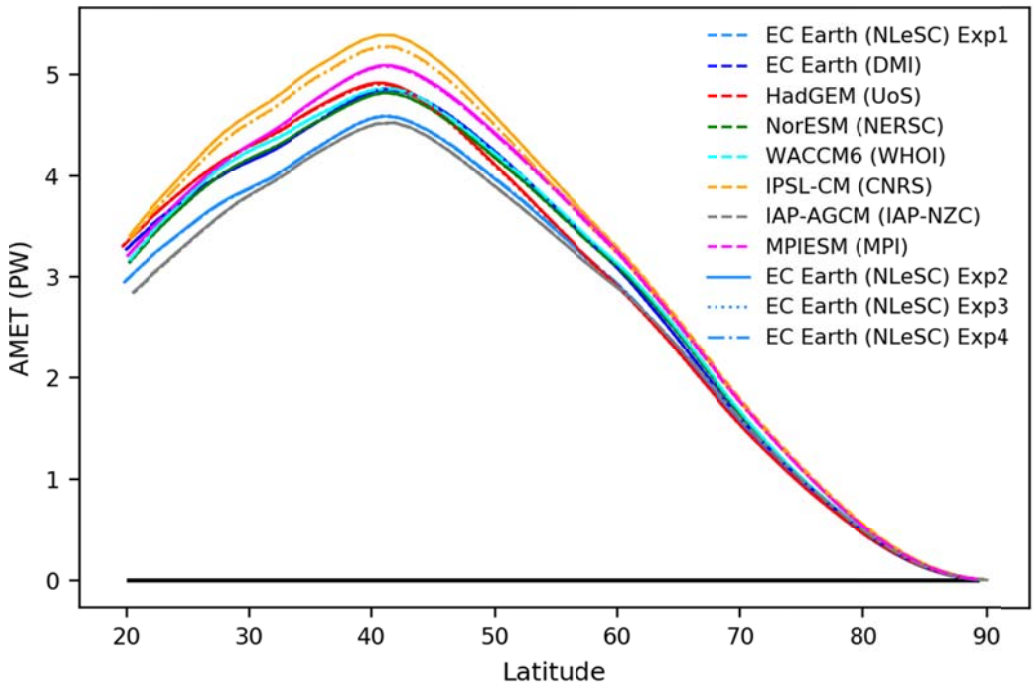

Figure 13 Mean atmospheric meridional energy transport over the entire time span at different latitudes from coordinated experiments. Only the ensemble means are shown in this figure. Results from control runs (Exp1, dashed line), simulations with fixed sea ice variation (Exp2, solid line), simulations without PDO (Exp3, dotted line) and AMO (Exp4, dash-dot line) are included. The unit is Peta Watt.

The mean AMET as a function of latitude from coordinated experiments are given in figure 13. Only the ensemble means are included in this figure. The maximum AMET is located around 41-degree North. The maximum of ensemble mean AMET in all the experiments by each model is given in Table 1. In general, mean AMET as a function of latitude in the Northern Hemisphere, including the peak values of AMET, are similar in different experiments, but not among all the models. Most of the models show that the peak AMET ranges from 4.8 – 5.0 PW. EC-Earth model with high resolution (by NLeSC) and IAP-AGCM model provide a slightly low maximum AMET, which is about 4.5 PW. While AMET peaks at 5.3 PW in IPSL-CM model (see figure 13 and Table 1). In general, the models agree well on the climatology of AMET.

Table 1 The maximum of mean atmospheric meridional energy transport over the entire time span at different latitudes from coordinated experiments. Only the ensemble means are shown in this table.

Coordinated experiments	Maximum of mean AMET (PW)			
	Exp1	Exp2	Exp3	Exp4
EC Earth (NLeSC)	4.584	4.588	4.593	4.587
EC Earth (DMI)	4.848	4.850	4.857	4.853
NorESM (NERSC)	4.821	4.818	4.818	4.818
WACCM6 (WHOI)	4.852	4.854	4.863	4.856
HadGEM (UoS)	4.913	4.916	4.900	4.904
IAP-AGCM (IAP-NZC)	4.522	4.523	4.522	4.528
IPSL-CM (CNRS)	5.385	5.386	5.266	5.274
MPIESM (MPI)	5.081	5.089	5.076	5.078

Though the climatology of AMET is not sensitive to the variations of sea ice, PDO and AMO, the anomalies of AMET vary with them. The ensemble mean low frequency signals of AMET at 60 degree North are given in figure 14. A low pass filter with a running mean of 5 years is applied to all the time series. Figure 14b highlights that the AMET in Exp2 is smaller than the AMET in Exp1 before 2004 but becomes larger after 2004. This is consistent with the set-up of Exp2, which takes the climatology of sea ice from 1979 to 2013/2014/2015. The standard deviations of the zonal integral of AMET anomalies at 60-degree North are listed in Table 2. Except for EC Earth (NLeSC) and IPSL-CM models, the standard deviations of AMET anomalies at 60-degree North are similar for all four experiments in each model. However, the mean absolute differences of AMET anomalies at 60-degree North between Exp1 and Exp2-4 indicate that sea ice, PDO and AMO all have large impact on the energy transport at subpolar latitudes (figure 16). These mean absolute differences are of the same magnitude as the standard deviations of AMET anomalies. Again, the results provided by EC-Earth (NLeSC) and IPSL-CM in Exp3 and Exp4 are different from the results given by other models. This might be related to their spatial resolution.

Table 2 The standard deviation (std) of the zonal integral of AMET anomalies at 60-degree North from coordinated experiments. Only the ensemble means are included in the calculations.

Coordinated experiments	Standard Deviation of AMET anomalies at 60deg N (PW)			
	Exp1	Exp2	Exp3	Exp4
EC Earth (NLeSC)	0.060	0.058	0.125	0.131
EC Earth (DMI)	0.061	0.057	0.058	0.058
NorESM (NERSC)	0.079	0.077	0.078	0.082
WACCM6 (WHOI)	0.068	0.057	0.061	0.062
HadGEM (UoS)	0.071	0.074	0.082	0.085
IAP-AGCM (IAP-NZC)	0.054	0.052	0.055	0.056
IPSL-CM (CNRS)	0.043	0.044	0.373	0.369
MPIESM (MPI)	0.067	0.072	0.067	0.081

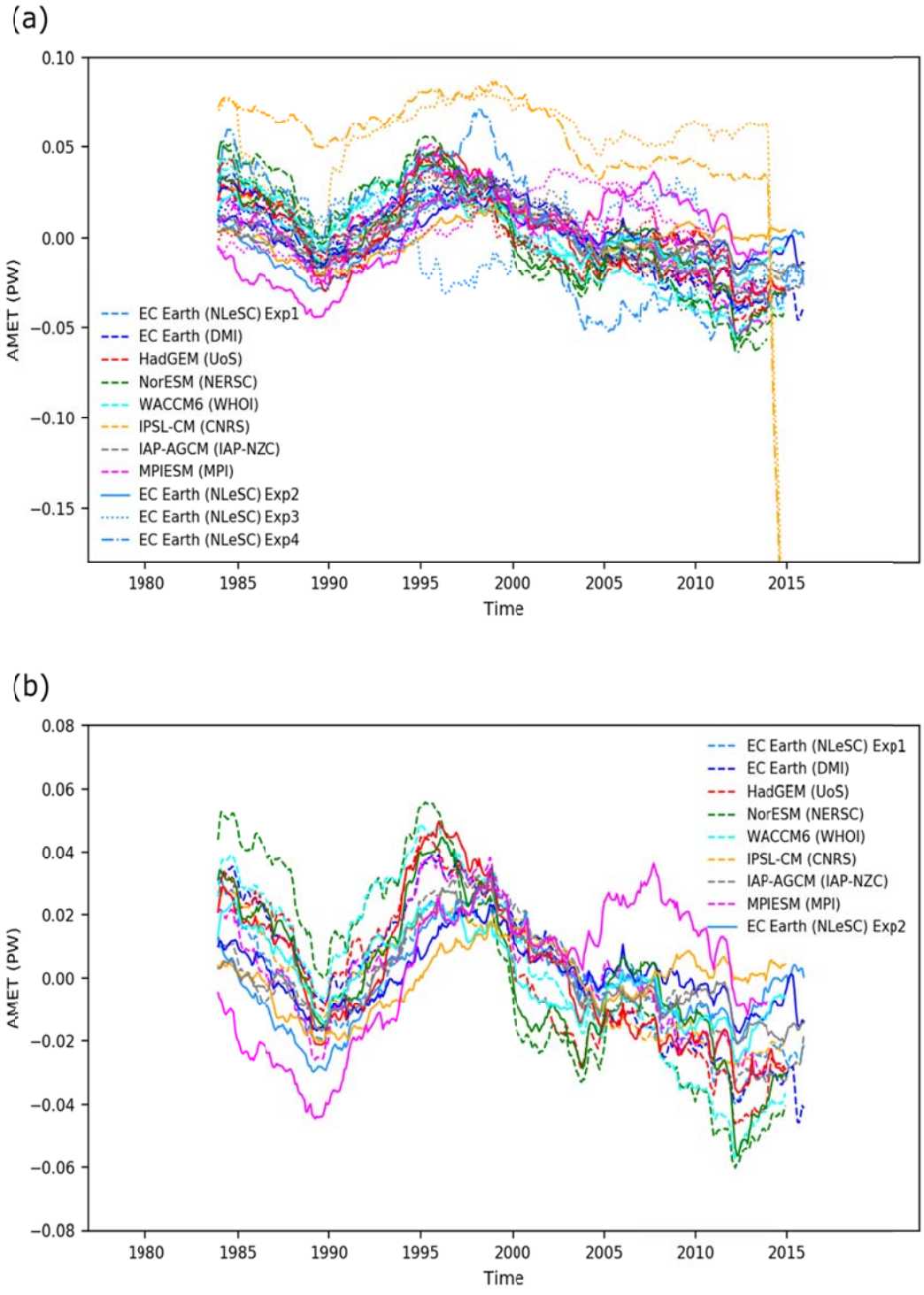

Figure 14 Low frequency time series of the zonal integral of AMET anomalies at 60 degrees North from coordinated experiments. Only the ensemble means are shown in this figure. Results from Exp1 (dashed line), Exp2 (solid line), Exp3 (dotted line) and Exp4 (dash-dot line) are included in (a). A comparison between results from Exp1 and Exp2 is given in (b). A running mean of 5 years is taken as the low pass filter. The unit is Peta Watt.

Moreover, the trend of AMET at each latitude in each experiment is given in figure 15. Strong negative trends of AMET between 50 degrees North and 60 degrees North are observed in almost all the experiments by each model (figure 15b). Generally, the trend of AMET in Exp2 is weaker than that in other experiments. This indicates that sea ice melting can potentially increase the northward heat transport in the atmosphere. The influence of PDO and AMO is relatively small on the trend of AMET compared to Exp1. Besides, large negative trends in the South Hemisphere around 40-degree South can be found in figure 15a.

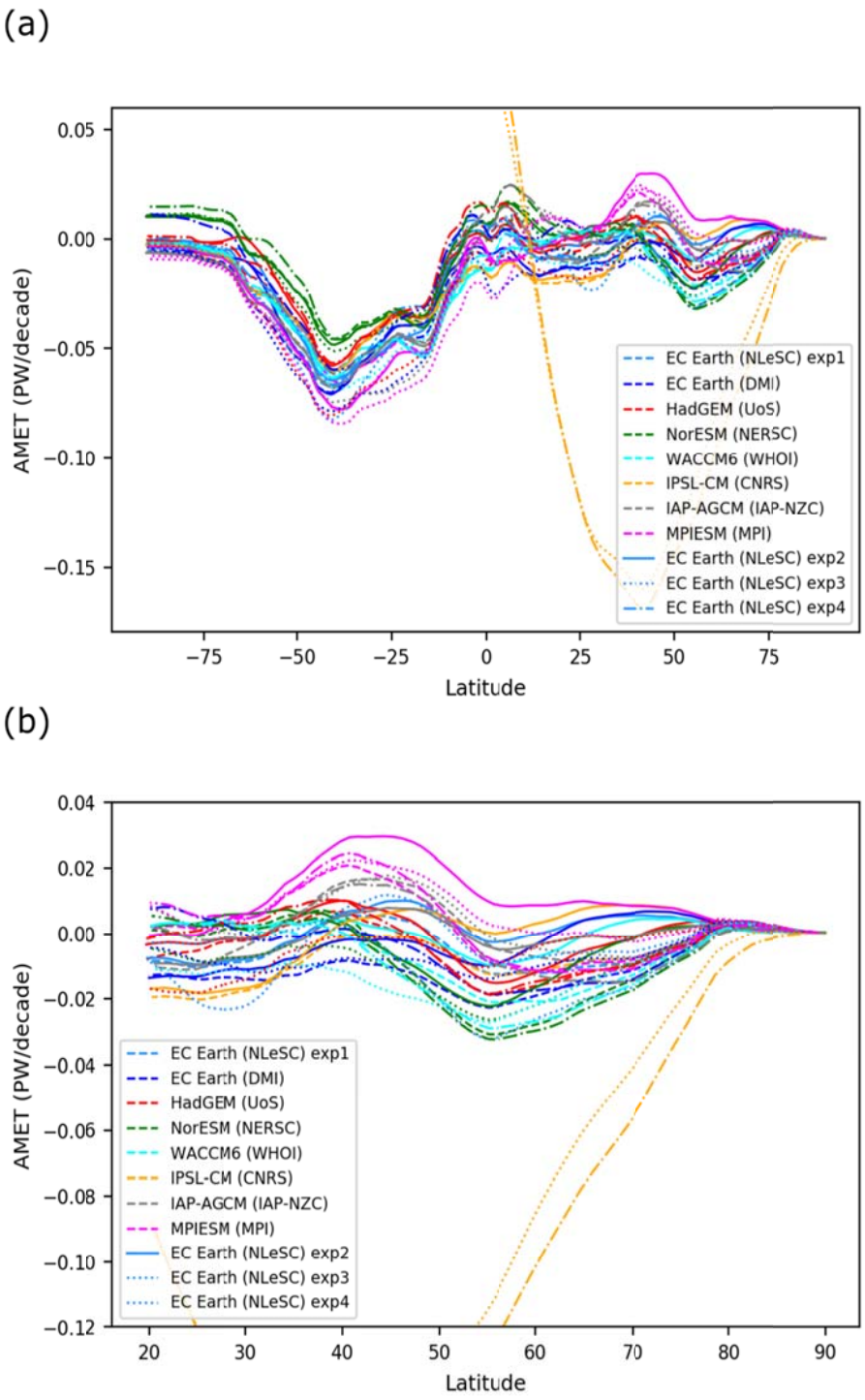

Figure 15 Trend of atmospheric meridional heat transport over the entire time span at different latitudes from coordinated experiments. Results from Exp1 (dashed line), Exp2 (solid line), Exp3 (dotted line) and Exp4 (dash-dot line) are included. The trend of AMET as a function of latitude across the entire globe is shown in (a) and the trend of AMET in the Northern Hemisphere is highlighted in (b). The unit is Peta Watt / decade.

To further evaluate the impact of sea ice and large-scale climate patterns on the local heat budget in the Arctic, we study the variation of turbulent fluxes at the surface in the Arctic. The trend of surface turbulent fluxes in the Arctic in each experiment is shown in figure 16. The results are based on the ensemble mean surface sensible and latent heat fluxes by each model. In Exp1, strong negative trends of surface turbulent fluxes are observed on the Greenland Sea, the Barents Sea, the Kara Sea and the Baffin Bay. There are also places with positive trends across the Greenland Sea and the Barents Sea. However, with Exp2, the trends of turbulent fluxes become much smaller in these regions. Such changes with less active turbulent fluxes in the Arctic are expected since the air-sea interaction is hindered by the presence of fixed sea ice. This also indicates the important role of the Arctic sea ice in terms of the heat budget and supports the fact that the northward energy transport will be impacted by sea ice (e.g. figure 14b). Besides, PDO and AMO have insignificant impact on the trend of surface turbulent fluxes in the Arctic, which is consistent with the results obtained in figure 15.

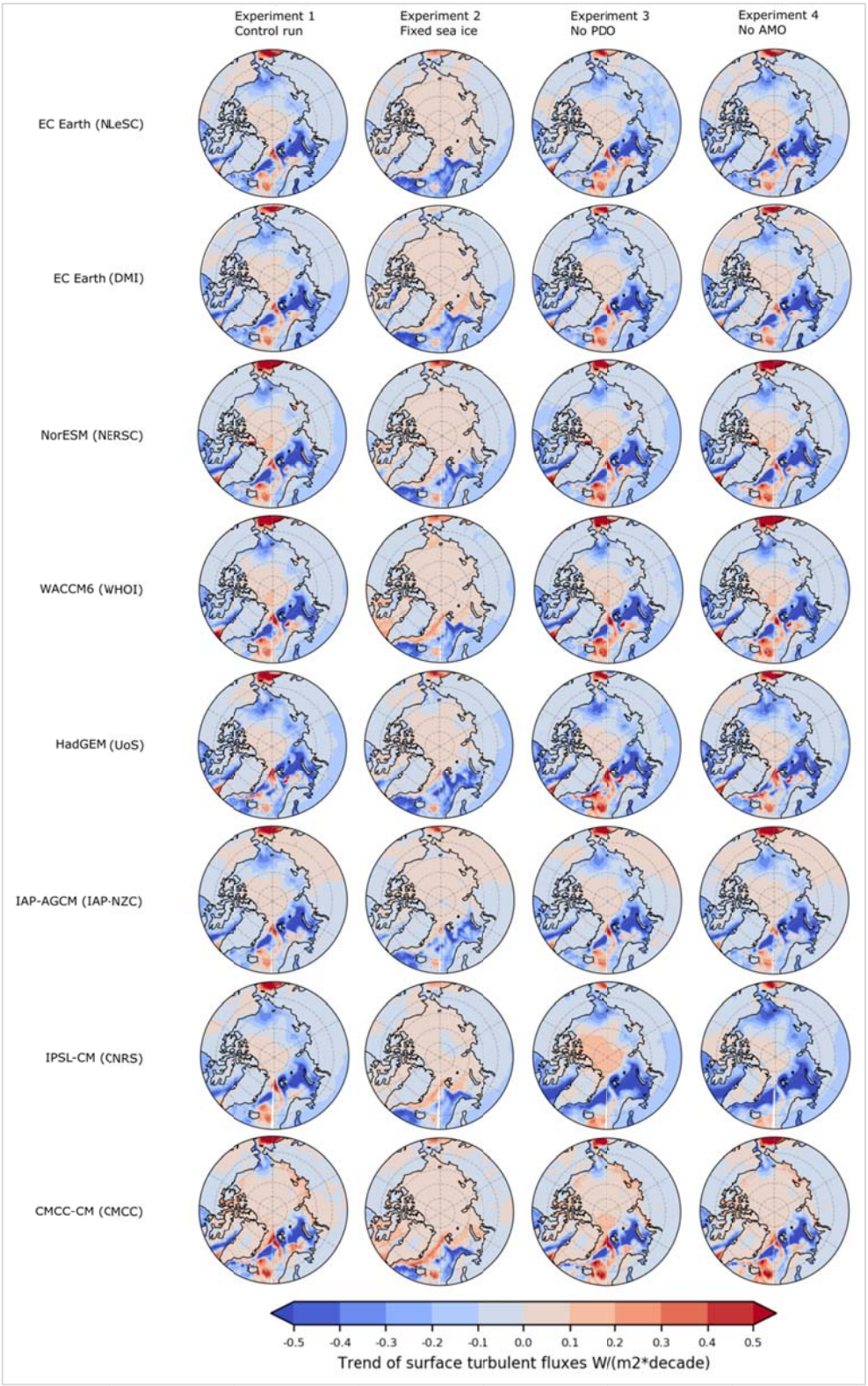

Figure 16 Trend of net surface fluxes over the entire time span in the polar cap from coordinated experiments. The results are based on ensemble means. Results from Exp1 (dashed line), Exp2 (solid line), Exp3 (dotted line) and Exp4 (dash-dot line) are included. The unit is Watt per square meter per decade.

To summarize:

- The influences of the Arctic sea ice variation, the PDO and AMO on the climatology of AME in the Northern Hemisphere are small in most of the models.
- The Arctic sea ice has a strong impact on AMET anomalies at subpolar regions and the energy budget in the Arctic, in terms of both the trend of AMET anomalies and the turbulent fluxes.
- The PDO and AMO, have a strong impact on the variability of AMET anomalies, but relatively small impact on the trend of AMET anomalies and surface turbulent fluxes at high latitudes.

Atmosphere circulation response to the Arctic sea ice decline in a regional climate model (Leading partner: Russian partner IAP)

Ensemble simulations with COSMO-CLM regional atmospheric model for the domain restricted by Northern Eurasia and major part of the Arctic Ocean were performed to test the sensitivity of the atmospheric circulation to the strong winter sea ice reduction in the Barents and Kara Seas in the last three decades. Simulations were performed for high and low sea ice concentrations in the Barents and Kara Seas and, for both cases, under conditions of strong and weak zonal circulations prescribed at the lateral domain boundaries. The simulation setup aimed to test the possibility of the Warm Arctic – Cold Siberia (WACS) response to the winter sea ice reduction on a continental scale without involving troposphere-stratosphere interaction and planetary-scale wave disturbances, and to assess the dependence of the response on the background zonal circulation conditions imposed at the lateral boundaries of the simulation domain.

The analysis of the ensemble mean climate response to SIC reduction revealed that the most significant changes occurred in February. Figure 17 shows simulated surface air temperature (SAT) and sea level pressure (SLP) response to the imposed sea ice reduction under conditions of strong and weak zonal flow. For both zonal flow conditions, the local SAT response is characterized by an expectedly strong warming in the area of sea ice retreat exceeding 5°C (Figure 17a,c). The remote large-scale temperature changes have noticeable differences. In case of the strong zonal flow, SAT response consists of moderate but statistically significant continental-scale warming from about 10E to 100E, excluding the eastern Siberia and southern Siberia, where some weak cooling is simulated with small spots of statistically significant changes. More enhanced SAT increase (up to 2°C) is found in the region south of the Barents and Kara Seas' coast. In case of the weak zonal flow, the warming over Northern Eurasia (NE) is more confined to statistically significant warming in the northern continental areas from about 20E to 60E. Importantly, there is a statistically significant cooling over large areas in the southern Siberia with additional stripe of negative SAT anomalies in the north-east Siberia (figure 17d). This pattern bears quite some resemblance with the observed SAT anomalies in NE in the beginning of the 21st century (Figure 17e).

SAT response differences are related to low-troposphere-circulation response illustrated in terms of SLP changes. Under the strong zonal flow conditions, SIC reduction results in practically domain-wide SLP decrease with strongest changes over the forcing region in the north-eastern Barents and western Kara Seas and fading out signal strength with increasing distance. Such a response to lower boundary heating related to sea ice reduction was found in several modeling studies (e.g., Alexander et al., 2004; Deser et al., 2004; Peings and Magnusdottier 2014) and is consistent with theoretical models of the linear baroclinic response to extratropical thermal forcing (e.g., Hoskins and Karoly, 1981; Kushnir et al. 2002).

In conditions of the weakened westerlies, the SLP response is drastically different. Large-scale positive SLP anomaly reaching 2 hPa is now simulated to the south of the Kara Sea. This positive SLP response explains the SAT cooling by anomalous northerly cold air advection. The SLP changes are statistically significant only in restricted areas in the southern Siberia, which is related to strong inter-ensemble variability (to be discussed later) and relatively small ensemble size. SLP changes over the Barents and Kara Seas in case of the weak zonal flow are statistically insignificant and consist of relatively weak (generally not more than 1 hPa) negative anomaly around Novaya Zemlya and Franz Josef Land (directly over negative SIC area) with adjacent positive anomaly centered over Nord Cap (figure 1d). The positive SLP anomaly in Central Siberia is accompanied by a negative anomaly in the Eastern Europe from the Baltic Sea to the Black Sea with statistically significant changes over the Black Sea region, forming a west-east pressure dipole. Such a response is much weaker but in a qualitative agreement with the observed SLP anomaly in the beginning of the 21st century with a strong SLP increase in the Central Siberia accompanied by decreased pressure to the west (figure 17f).

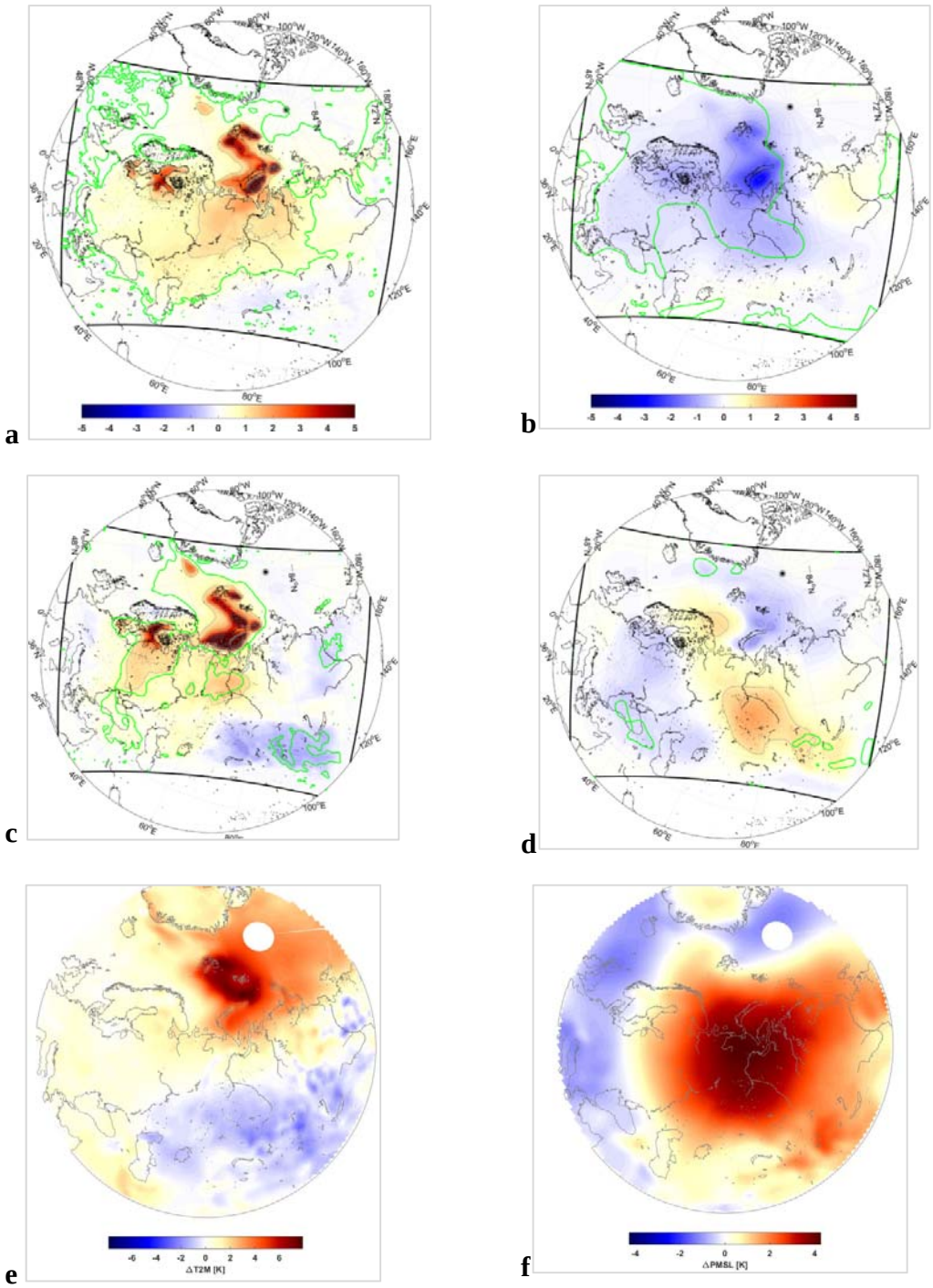

Figure 17 Simulated ensemble mean February SAT (a,b, in °C) and SLP (b,d, in hPa) response to sea ice reduction under weak (a,c) and strong (c,d) zonal wind conditions. Green lines encompass statistically significant changes at 90% confidence level. Thick black lines denote simulation domain borders. Also shown are SAT (e) and SLP (f) changes from ERA-Interim reanalysis averaged for the period 2005-2018 relative to 1981-2010 mean.

The magnitude of the WACS response is underestimated in comparison to the corresponding observed changes. Such underestimation is a systematic feature of global AGCMs that may stem, in particular, from the lack of ocean-ice-atmosphere coupling and can be treated by dedicated statistical methods to extract SIC-related signal (Mori et al., 2019).
Two different types of response, local baroclinic and large-scale equivalent barotropic, or shallow ridge and downstream mid-troposphere trough (that were revealed by the vertical response structure, not shown), are consistent with previously described regional and large-scale responses to SIC reduction in global AGCMs (e.g., Alexander et al., 2004; Deser et al., 2004; Peings and Magnusdottier 2014). Our results show that the atmosphere circulation and temperature WACS response to SIC reduction, may by nature be similar to the response to mid-latitude warm SST anomaly (Peng et al., 1997), and crucially depends on the background circulation.

Main results achieved

Arctic amplification metrics

The surface air temperature (SAT) anomalies, trends and variability have been used to quantify the Arctic amplification (AA). The use of different metrics, as well as the choice of dataset to use can affect conclusions about the magnitude and temporal variability of AA. Here we review the established metrics of AA to see how well they agree upon the temporal signature of AA, such as the multi-decadal variability, and assess the consistency in these metrics across different commonly-used datasets which cover both the early and late 20th century warming in the Arctic. We find the NOAA 20th Century Reanalysis most closely matches the observations when using metrics based upon SAT trends (A2), variability (A3) and regression (A4) of the SAT anomalies, and the ERA 20th Century Reanalysis is closest to the observations in the SAT anomalies (A1) and variability of SAT anomalies (A3). However, there are large seasonal differences in the consistency between datasets. Moreover, the largest differences between the century-long reanalysis products and observations are during the early warming period., likely due to the sparseness of the observations in the Arctic at that time. In the modern warming period, the high density of observations strongly constrains all the reanalysis products, whether they include satellite observations or only surface observations. Thus, all the reanalysis and observation products produce very similar magnitudes and temporal variability in the degree of AA during the recent warming period (Davy et al., 2018).

Sea ice free Arctic contributes to the projected warming minimum in North Atlantic

Projected global warming is not spatially uniform and one of the minima in warming occurs in the North Atlantic (NA). Several models from the Coupled Model Intercomparison Project Phase 5 even projected a slight NA cooling in 2081–2100 relative to 1986–2005. Here we show that, by coupled model simulations, an autumn (September to November) sea-ice free Arctic contributes to the NA warming minimum by weakening the Atlantic meridional overturning circulation (Suo et al., 2017).

The atmosphere-only model coordinated experiments were re-designed and finalized.

The coordinated experiments were completed by the nine of ten atmosphere-only models

Joint analysis on the coordinated experiments by the nine of ten atmosphere-only models is ongoing.

The WP3 team has been very active in disseminating their progress and results and have a record of more than 15 **dissemination activities** listed for this period. The list of activities ranges from invited talks to major events (EC workshop ''Arctic Workshop of the Transatlantic Ocean research alliance'', GREENICE project meeting, AMAP Meeting on contributions to the IPCC. PAMIP workshop in UK), and the organisation of a joint workshop with the project INTAROS.

Publications: 4 publications acknowledging the project have been accepted and published in open access. The full list of publications is available at the end of this deliverable.

Progress beyond the state of the art

The numbers of simulations and participation models that are produced within WP3 is unprecedented, it will not only allow a better estimation of the impacts of the warming Arctic, but will also reveal the role of the Atlantic and Pacific decadal variability. We believe this is the first time to have 9 atmosphere-only models to investigate the Arctic warming with coordinated experiments. The designed and completed experiments to separate the impacts of Pacific and Atlantic multi-decadal variabilities have not been performed before.

An original mechanism has been proposed to relate the warming Arctic to the cooling North Atlantic expected in global warming conditions. The Atlantic cooling can be partly explained by an atmospheric-oceanic bridge.

Warm Pacific can intensify the Arctic warming: Multi-model simulations from Blue-Action showed that the transition from warm Pacific to cold Pacific (Pacific Decadal Oscillation from positive phase to negative phase) during 1979-2013 damped the Arctic warming. The Arctic warming likely will be intensified in the forthcoming decades given the PDO switched to positive phase since 2014.

Impact

The work presented in this document contributes to the following expected impact of Blue-Action.

"Improve capacity to predict the weather and climate of the Northern Hemisphere, and make it possible to better forecast of extreme weather phenomena": Improved representation of process specific to the Arctic will be emphasized in deliverable D3.5. The present deliverable contributes to the improved representation of Arctic-lower latitude linkages by atmospheric bridge (coordinated experiments by 9 atmosphere-only models) and by atmosphere-ocean coupled pathway (individual coupled model simulation).

Lessons learned and Links built

Synergies with other projects: WP3 is in close communication with Blue-Action WP4 "Enhancing the capacity of seasonal-to-decadal predictions in the Arctic and over the Northern Hemisphere". WP3 is also in close contact with the **JPI Climate/ERA4CS funded project InterDec** http://www.jpi-climate.eu/2015projects/interdec, led by Daniela Matei/MPI-M (also lead of Blue-Action WP4). In this project, coordinated experiments will be performed to investigate the impact of the tropical sea surface temperature variation on the Arctic warming.

Synergies with H2020 project INTAROS: WP3 Blue-Action and INTAROS workshop organised a **Joint INTAROS/Blue-Action workshop at Nansen-Zhu Center on 18 April 2018 on "Arctic monitoring, modeling and Arctic teleconnection and prediction"**. Organisers of the workshop were Stein Sandven (INTAROS) and Yongqi Gao (INTAROS & WP3 Blue-Action). Chinese partners in INTAROS contribute with their in-situ data, Chinese satellite data and sea ice prediction. The Chinese partner in Blue-Action, Institute of Atmospheric Physics of the Chinese Academy of Sciences, contributes with the coordinated experiments in WP3 and focuses more on the impact of Arctic warming on the climate and extreme weather in particular over the East Asia. The Chinese partners in INTAROS are the Polar Research Institute of China in Shanghai, National Marine Environment Forecasting Center, Institute of Remote Sensing and Digital Earth, Chinese Academy of Sciences.

Complementary funding for the non-EU Partners: The Institute of Atmospheric Physics of the Chinese Academy of Sciences is an official partner in the Blue-Action project and consortium, but does not receive EU funding through the project. An application of the Institute to the Ministry of Science and Technology in China (MOST) was funded, thus **Nansen-Zhu is a fully fledged partner in Blue-Action but funded by Chinese funds.**

Russian partner was not able to perform the coordinated experiments due to infrastructure problem. Instead, the Russian partner contribute the study of Arctic warming impact by using regional model.

Contribution to the top level objectives of Blue-Action

This deliverable contributes to the achievement of all the objectives and specific goals indicated in the Description of the Action, part B, Section 1.1: http://blue-action.eu/index.php?id=4019

Objective 1 Improving long range forecast skill for hazardous weather and climate events
The completed atmospheric coordinated model experiments will allow investigating the hazardous weather and climate events with improved sampling. The simulations were by the surface boundary conditions used by the High Resolution CMIP6 panel. Such high resolution will provide an improved estimation of impacts of the variability modes.

Objective 2 Enhancing the predictive capacity beyond seasons in the Arctic and the Northern Hemisphere
The climate linkage through atmospheric bridge between the Arctic warming and the lower-latitudes are investigated with coordinated numerical experiments by multi-models (ongoing).

The identified responsible mechanisms to climate linkage have the potential to enhance predictive capacity beyond seasons in the Arctic and the Northern Hemisphere. As an example, Suo et al. (2017), by single model experiments, showed that the melting of autumn Arctic sea ice can slow-down the winter warming over the North Atlantic.

Objective 3 Quantifying the impact of recent rapid changes in the Arctic on Northern Hemisphere climate and weather extremes

The completed atmospheric multi model experiments of Blue-Action will allow investigating the impacts of the observed sea ice decline as well as the influence of the main mode of natural climate variability. A main focus will be on the impacts of the Atlantic and Pacific Multidecadal Variability. Such impacts are small compared to the internal atmospheric variability occurring in the Northern hemisphere. Most of the partners produced large ensemble of experiments with 20 members, which will provide an unprecedented and improved signal to noise ratio. This is a requisite in order to establish robust impact of the rapid Arctic change on the weather and climate and quantify the impact onto the hazardous weather events.

Objective 4 Improving the description of key processes controlling the impact of the polar amplification of global warming in prediction systems

The analysis on the completed atmospheric multi model experiments of Blue-Action will identify the key processes controlling the impact of the polar amplification of global warming and potentially contribute to the improved description of the key processes.

Objective 5 Optimizing observational systems for predictions

The full ensemble of atmospheric coordinated experiments will be analysed to investigate the mechanism of the recent climatic extremes and their links with the Arctic Ocean and sea ice conditions. The ongoing analysis on the multi-model coordinated experiments will help to pinpoint the region of the Arctic which have the largest impacts on cold air outbreaks or heat waves.

Roles of the Atlantic and Pacific in modulation of the Arctic warming and its impact will be investigated by the coordinated experiments by multi-models. The results have the potential to better design the observational systems for predictions over the Arctic, for this reason, a joint INTAROS-Blue-Action workshop was organised to this respect on 18 April 2018 on **'Arctic monitoring, modeling and Arctic teleconnection and prediction'** at Nansen-Zhu Center, Beijing (CHN).

Objective 6 Reducing and evaluating the uncertainty in prediction systems

The impact of Arctic warming (by change in Arctic sea ice in Blue-Action) with the coordinated experiments by multi-models can be used to evaluate the uncertainty in prediction system.

Objective 8 Transferring knowledge to a wide range of interested key stakeholders, including the scientific community, via intensive dissemination activities, organisation of joint workshops with other projects, and scientific publications.

References (Bibliography)

These are the papers or publications we consulted during the research.

- Alexander, M. A., U. S. Bhatt, J. E. Walsh, M. S. Timlin, J. S. Miller, and J. D. Scott, 2004: The atmospheric response to realistic Arctic sea ice anomalies in an AGCM during winter. J. Climate, 17, 890–905.
- Banzon, V., Smith, T. M., Chin, T. M., Liu, C., & Hankins, W. (2016). A long-term record of blended satellite and in situ sea-surface temperature for climate monitoring, modeling and environmental studies. Earth Syst. Sci. Data, 8, 165-176.
- Boer, G. J., Smith, D. M., Cassou, C., Doblas-Reyes, F., Danabasoglu, G., Kirtman, B., Kushnir, Y., Kimoto, M., Meehl, G. A., Msadek, R., Mueller, W. A., Taylor, K. E., Zwiers, F., Rixen, M., Ruprich-Robert, Y., & Eade, R. (2016). The Decadal Climate Prediction Project (DCPP) contribution to CMIP6. Geosci. Model Dev., 9, 3751-3777, https://doi.org/10.5194/gmd-9-3751-2016.
- Comiso, J. C. (2017). Bootstrap Sea Ice Concentrations from Nimbus-7 SMMR and DMSP SSM/I-SSMIS, Version 3. Boulder, Colorado USA. NASA National Snow and Ice Data Center Distributed Active Archive Center, doi: https://doi.org/10.5067/7Q8HCCWS4I0R.
- Deser C., Magnusdottir G., Saravanan R. and Phillips A. 2004 The effects of North Atlantic SST and sea ice anomalies on the winter circulation in CCM3: II. Direct and indirect components of the response J. Clim. 17 877–89.
- Frankignoul, C., Gastineau, G., & Kwon, Y. O. (2017). Estimation of the SST Response to Anthropogenic and External Forcing and Its Impact on the Atlantic Multidecadal Oscillation and the Pacific Decadal Oscillation. J. Climate, 30, 9871–9895, https://doi.org/10.1175/JCLI-D-17-0009.1.
- Haarsma, R. J., Roberts, M. J., Vidale, P. L., Senior, C. A., Bellucci, A., Bao, Q., Chang, P., Corti, S., Fučkar, N. S., Guemas, V., von Hardenberg, J., Hazeleger, W., Kodama, C., Koenigk, T., Leung, L. R., Lu, J., Luo, J. J., Mao, J., Mizielinski, M. S., Mizuta, R., Nobre, P., Satoh, M., Scoccimarro, E., Semmler, T., Small, J.,& von Storch, J. S. (2016). High Resolution Model Intercomparison Project (HighResMIP v1.0) for CMIP6. Geosci. Model Dev., 9, 4185-4208, https://doi.org/10.5194/gmd-9-4185-2016.
- Hazeleger, W., Wang, X., Severijns, C., Stefa¢nescu, S., Bintanja, R., Sterl, A., Wyser, K., Semmler, T., Yang, S., van den Hurk, B., van Noije,T., van der Linden, E., & van der Wiel, K. (2012). ECEarth V2. 2: description and validation of a new seamless earth system prediction model. Clim. Dyn., 39, 2611–2629, https://doi.org/10.1007/s00382-011-1228-5.
- Henley, B. J., Gergis, J., Karoly, D. J., Power, S., Kennedy, J., & Folland, C. K. (2015). A tripole index for the interdecadal Pacific oscillation. Clim. Dyn., 45, 3077-3090.
- Hoskins, B. J., and D. J. Karoly, 1981: The steady linear response of a spherical atmosphere to thermal and orographic forcing. J. Atmos. Sci., 38, 1179–1196.
- Hurrell, J. W., Hack, J. J., Shea, D., Caron, J. M., & Rosinski, J. (2008). A new sea surface temperature and sea ice boundary dataset for the Community Atmosphere Model. J. Climate, 21, 5145–5153, https://doi.org/10.1175/2008JCLI2292.1.
- Screen, J. A. (2017). Simulated atmospheric response to regional and Pan-Arctic sea-ice loss. J. Climate, 30, 3945–3962,doi:10.1175/JC¬LI-D-16-0197.1.

- Ting, M., Kushnir, Y., Seager, R., & Li, C. (2009). Forced and internal twentieth-century SST trends in the North Atlantic. J. Climate, 22, 1469–1481, https://doi.org/10.1175/2008JCLI2561.1.
- Titchner, H. A., & Rayner, N. A. (2014). The Met Office Hadley Centre sea ice and sea surface temperature data set, version 2: 1. Sea ice concentrations. J. Geophys. Res. Atmos., 119, 2864–2889, doi: 10.1002/2013JD020316.
- Trenberth, K. E., & Shea, D. J. (2006). Atlantic hurricanes and natural variability in 2005. Geophys. Res. Lett., 33, L12704, doi:10.1029/2006GL026894.
- Walters, D., Baran, A., Boutle, I., Brooks, M., Earnshaw, P., Edwards, J., Furtado, K., Hill, P., Lock, A., Manners, J., Morcrette, C., Mulcahy, J., Sanchez, C., Smith, C., Stratton, R., Tennant, W., Tomassini, L., Van Weverberg, K., Vosper, S., Willett, M., Browse, J., Bushell, A., Dalvi, M., Essery, R., Gedney, N., Hardiman, S., Johnson, B., Johnson, C., Jones, A., Mann, G., Milton, S., Rumbold, H., Sellar, A., Ujiie, M., Whitall, M., Williams, K., & Zerroukat, M.: The Met Office Unified Model Global Atmosphere 7.0/7.1 and JULES Global Land 7.0 configurations. Geosci. Model Dev. Discuss., https://doi.org/10.5194/gmd-2017-291, in review, 2017.
- Frankignoul, C., Chouaib, N., & Liu, Z. (2011). Estimating the observed atmospheric response to SST anomalies: maximum covariance analysis, generalized equilibrium feedback assessment, and maximum response estimation. *Journal of Climate*, *24*(10), 2523-2539.
- Frankignoul, C., Sennéchael, N., & Cauchy, P. (2014). Observed atmospheric response to cold season sea ice variability in the Arctic. *Journal of Climate*, *27*(3), 1243-1254.
- Gastineau, G., García-Serrano, J., & Frankignoul, C. (2017). The influence of autumnal Eurasian snow cover on climate and its link with Arctic sea ice cover. *Journal of Climate*, *30*(19), 7599-7619.
- King, M. P., Hell, M., & Keenlyside, N. (2016). Investigation of the atmospheric mechanisms related to the autumn sea ice and winter circulation link in the Northern Hemisphere. *Climate dynamics*, *46*(3-4), 1185-1195.
- Kug, J. S., Jeong, J. H., Jang, Y. S., Kim, B. M., Folland, C. K., Min, S. K., & Son, S. W. (2015). Two distinct influences of Arctic warming on cold winters over North America and East Asia. *Nature Geoscience*, *8*(10), 759.
- Kushnir, Y., W. A. Robinson, I. Bladé, N. M. J. Hall, S. Peng, and R. Sutton, 2002: Atmospheric GCM response to extratropical SST anomalies: Synthesis and evaluation. J. Climate, 15, 2233–2256.
- Mori, M., Kosaka, Y., Watanabe, M., Nakamura, H., & Kimoto, M. (2019). A reconciled estimate of the influence of Arctic sea-ice loss on recent Eurasian cooling. Nature Climate Change, 9(2), 123–129. https://doi.org/10.1038/s41558-018-0379-3.
- Mudryk, L. R., Kushner, P. J., Derksen, C., & Thackeray, C. (2017). Snow cover response to temperature in observational and climate model ensembles. *Geophysical Research Letters*, *44*(2), 919-926.
- Ogawa, F., Keenlyside, N., Gao, Y., Koenigk, T., Yang, S., Suo, L., ... & Omrani, N. E. (2018). Evaluating impacts of recent Arctic sea ice loss on the northern hemisphere winter climate change. *Geophysical Research Letters*, *45*(7), 3255-3263.
- Peings, Y., Douville, H., Alkama, R., & Decharme, B. (2011). Snow contribution to springtime atmospheric predictability over the second half of the twentieth century. *Climate Dynamics*, *37*(5-6), 985-1004.

- Peings, Y., and G. Magnusdottir, 2014: Response of the wintertime Northern Hemisphere atmospheric circulation to current and projected Arctic sea ice decline: A numerical study with CAM5. J. Climate, 27, 244–264.
- Peng, S., W. A. Robinson, and M. P. Hoerling, 1997: The modeled atmospheric response to midlatitude SST anomalies and its dependence on background circulation states. J. Climate, 10, 971–987, https://doi.org/10.1175/1520-0442.
- Screen J.A. and Francis J.A. (2016): Contribution of sea-ice loss to Arctic amplification is regulated by Pacific Ocean decadal variability. Nature Climate Change. http://dx.doi.org/10.1038/nclimate3011
- Svendsen, L., Keenlyside, N., Bethke, I., Gao, Y.Q., Omrani, N.E., (2018): Pacific contribution to the early 20th century warming in the Arctic. Nature Climate Change. http://dx.doi.org/ 10.1038/s41558-018-0247-1
- Zhang, Y., Li, T., & Wang, B. (2004). Decadal change of the spring snow depth over the Tibetan Plateau: The associated circulation and influence on the East Asian summer monsoon. *Journal of Climate*, *17*(14), 2780-2793.

Dissemination and exploitation of Blue-Action results

Dissemination activities

Type of dissemination activity	Name of the scientist (institution), title of the presentation, event	Place and date of the event (keep the formatting!)	Estimated budget	Type of Audience	Estimated number of persons reached	Link to Zenodo upload
Participation to a conference	Guillaume Gastineau (CNRS): Climate influence of autumnal Eurasian snow cover and its links with sea ice cover	Berlin (DE), 18-20 January 2017	See the form C of the partner involved.	Scientific Community (higher education, Research)	70	https://doi.org/10.5281/zenodo.1288554
Participation to workshop	Yongqi Gao (NERSC): Arctic amplification and its potential linkage with Eurasian climate, at the International Workshop on Cryospheric Change and Sustainable Development	Lanzhou, (CHN), 1-2 August 2017	See the form C of the partner involved.	Scientific Community (higher education, Research)	200	http://doi.org/10.5281/zenodo.1287684
Participation to a seminar	Claude Frankignoul (CNRS) presentation “The wintertime atmospheric response to the Atlantic meridional overturning circulation, and its link to the Atlantic Multidecadal Oscillation” at the Seminar in Woods Hole Oceanic Institute.	Woods Hole (USA) 5 Sept 2017	See the form C of the partner involved.	Scientific Community (higher education, Research)	40	https://doi.org/10.5281/zenodo.1187058

Other (Poster)	Rohit Ghosh (MPIM), The atmospheric pathway between AMV and European summer climate in an atmospheric model , at the Summer school " at the Globally Observed Teleconnections in a Hierarchy of Atmospheric Models (GOTHAM)" at PIK Potsdam	Potsdam (DE) 18-22 September 2017	See the form C of the partner involved.	Scientific Community (higher education, Research)	30	https://zenodo.org/record/1296196#.XY0pGpMzbfY
Participation to a conference	Guillaume Gastineau (CNRS), at the GREENICE final meeting : Snow Cover and Sea-Ice Impacts and their Links in coordinated experiments	Reykjavik (IS), 17-18 October 2017	See the form C of the partner involved.	Scientific Community (higher education, Research)	20	https://doi.org/10.5281/zenodo.1288520
Participation to a workshop	Guillaume Gastineau, at the Second Workshop on AMAP contributions to the IPCC (remotely) : Blue Action Project Overview	Helsinki (FI), 6 March 2018	See the form C of the partner involved.	Scientific Community (higher education, Research)	50	https://doi.org/10.5281/zenodo.1288560
Other (Poster)	Lingling Suo (NERSC): Sea-ice free Arctic contributes to the projected warming minimum in the North Atlantic (Poster), at EGU	Vienna (AT), 8-13 April 2018	See the form C of the partner involved.	Scientific Community (higher education, Research)	>500	https://zenodo.org/record/1287765#.Wx-78kxuLu4
Organization of a workshop for INTAROS and Blue-Action	Yongqi Gao (NERSC): Introduction of Blue-Action	Beijing, (CHN), 18 April 2018	See the form C of the partner involved.	Scientific Community (higher education, Research)	30	https://www.zenodo.org/communities/blue-actionh2020
Other (Poster)	Jennifer Mecking (UoS/NOC): Impacts of Changing Sea Ice Cover on Northern Hemisphere Atmospheric Conditions, at EGU 2018	Vienna (AT) 8-13 April 2018	See the form C of the partner involved.	Scientific Community (higher education, Research)	>500	https://zenodo.org/record/1283379#.WxqQ0Kkh1Bx
Other (Poster)	Amélie Simon (CNRS) at "Arctic System Change Workshop": How to constrain the Arctic sea ice in a coupled model?	Boulder (USA) 9 – 12 April 2018	See the form C of the partner involved.	Scientific Community (higher education, Research)	70	https://doi.org/10.5281/zenodo.1287880
Participation to a conference	Yongqi Gao (NERSC) at International Workshop on Cryospheric Changes and their Regional and Global Impacts: Arctic Amplification and Eurasian Climate: Revisit. (invited talk)	Dunhuang (CHN), 31 July -August 1 2018	See the form C of the partner involved	Scientific Community (higher education, Research)	150	https://doi.org/10.5281/zenodo.3451250

Participation to a conference	Yongqi Gao (NERSC) at the 8th TPE workshop: Regional climate change: from pole to pole: Arctic warming and Eurasian climate: a short review. (invited talk)	Gothenburg (SE) 24-26 September 2018	See the form C of the partner involved	Scientific Community (higher education, Research)	70	10.5281/zenodo.3451274
Participation to a conference	Yongqi Gao (NERSC) at The Second International Science Forum of Scientific Organizations on the Belt and Road Initiative: Impact of Arctic warming: uncertainties, implications and prospects. (invited talk)	Beijing (CHN), 4-5 November 2018	See the form C of the partner involved	Scientific Community (higher education, Research)	80	https://doi.org/10.5281/zenodo.3238286
Participation to a conference	Liang, Y.-C., Y.-O. Kwon, C. Frankignoul, G. Danabasoglu, and S. Yeager: Atmospheric responses to Arctic sea ice loss in a high-top atmospheric general circulation model. AGU Fall Meeting	Washington D.C. (USA), 10-14 December 2018	See the form C of the partner involved	Scientific Community (higher education, Research)	50	http://doi.org/10.5281/zenodo.3455799
Participation to a conference	Yongqi Gao at Arctic Circle China Forum: Arctic Warming Impacts: Uncertainties, Implications and Prospects	Shanghai (CHN), 10-11 May 2019	See the form C of the partner involved	Scientific Community (higher education, Research)	30	10.5281/zenodo.3237502
Participation to a conference	Liang, Y.-C., Y.-O. Kwon, C. Frankignoul, G. Danabasoglu, and S. Yeager: Atmospheric responses to Arctic sea ice loss in a high-top atmospheric general circulation model. AMS 15th Conference on Polar Meteorology and Oceanography	Boulder (USA), 19-23 May 2019	See the form C of the partner involved	Scientific Community (higher education, Research)	50	http://doi.org/10.5281/zenodo.3455804
Participation to a workshop	Liang, Y.-C., Y.-O. Kwon, C. Frankignoul, G. Danabasoglu, and S. Yeager: Atmospheric responses to Arctic sea ice loss in a high-top atmospheric general circulation model. 2019 CESM Workshop	Boulder (USA), 17-19 June 2019	See the form C of the partner involved	Scientific Community (higher education, Research)	50	http://doi.org/10.5281/zenodo.3387707
Participation to a workshop	Liang, Y.-C., Y.-O. Kwon, C. Frankignoul, G. Danabasoglu, and S. Yeager: Atmospheric responses to Arctic sea ice loss in high-top Whole Atmospheric Community Climate Model version 6 (WACCM6). PAMIP Workshop	South Devon (UK), 25-27 June 2019	See the form C of the partner involved	Scientific Community (higher education, Research)	50	http://doi.org/10.5281/zenodo.3387703

Peer reviewed articles

Title	Authors	Publication	DOI	How much did you pay for the publication?	Status?	Open Access granted	Comments on embargo time imposed by the publisher
Sea-ice free Arctic contributes to the projected warming minimum in North Atlantic	Suo L.L., Gao Y.Q., Guo D., Bethke I.	Environmental Research Letters	doi: 10.1007/s00376-017-7029-y	See the form C of the partners.	Published on 16 December 2017	Yes	6 months
Arctic amplification metrics	Davy, R., Chen, L.L., Hanna, E.	International Journal of Climatology	Doi: 10.1002/joc.5675	See the form C of the partners.	Published 13 July 2018	Yes	6 months
Estimation of the SST Response to Anthropogenic and External Forcing and Its Impact on the Atlantic Multidecadal Oscillation and the Pacific Decadal Oscillation	Frankignoul F, Gastineau G and Kwon Y-O	Journal of Climate	doi.org/10.1175/JCLI-D-17-0009.1	See the form C of the partners.	Published	Yes	6 months
The influence of autumnal Eurasian snow cover on climate and its link with Arctic sea ice cover	Gastineau G, Garcia-Serrano J and Frankignoul C.	Journal of Climate	doi.org/10.1175/JCLI-D-16-0623.1	See the form C of the partners.	Published	Yes	6 months

Uptake by the targeted audiences

As indicated in the Description of the Action, the audience for this deliverable is *t*he general public (PU) is and is made available to the world via CORDIS.

This is how we are going to ensure the uptake of the deliverables by the targeted audiences:

- Scientific dissemination of results to conferences and workshops.
- Regular exchange with scientists working in other projects and initiatives (PAMIP, INTAROS…).
- Publication of results on scientific journals.